DRAFT

ANL/RE/RP--89482-Vol.3

RECEIVED
MAR 27 1996
OSTI

PRODIAG

Combined Expert System/Neural Network for Process Fault Diagnosis

Volume 3: APPLICATION

J. Reifman
J. E. Vitela
T. Y. C. Wei

DOES NOT CONTAIN
CONTROLLED INFORMATION
Name/Org.: Argonne National Laboratory (Apt #: 198972)
Date: January 9, 2026

September 1995

Protected CRADA Data
Pursuant to P.L. 101-189
DO NOT DISSEMINATE
DO NOT REPRODUCE
PROTECTED UNTIL Sep 2000

MASTER

Argonne National Laboratory
9700 South Cass Avenue
Argonne, Illinois 60439

DISTRIBUTION OF THIS DOCUMENT IS LIMITED
No Automatic Distribution or Announcement
Refer all Requests ANL

Protected CRADA Data
Pursuant to P.L. 101-189
DO NOT DISSEMINATE
DO NOT REPRODUCE

PROTECTED CRADA INFORMATION
This product contains Protected CRADA Information which was produced on Sept. 1995 under CRADA No. C920290[illegible] and is not to be further disclosed for a period of 5 years from the date it was produced except as expressly provided for in the CRADA.

DISCLAIMER

This report was prepared as an account of work sponsored by an agency of the United States Government. Neither the United States Government nor any agency thereof, nor any of their employees, makes any warranty, express or implied, or assumes any legal liability or responsibility for the accuracy, completeness, or usefulness of any information, apparatus, product, or process disclosed, or represents that its use would not infringe privately owned rights. Reference herein to any specific commercial product, process, or service by trade name, trademark, manufacturer, or otherwise does not necessarily constitute or imply its endorsement, recommendation, or favoring by the United States Government or any agency thereof. The views and opinions of authors expressed herein do not necessarily state or reflect those of the United States Government or any agency thereof.

DISCLAIMER

Portions of this document may be illegible in electronic image products. Images are produced from the best available original document.

TABLE OF CONTENTS

Protected CRADA Data
Pursuant to P.L. 101-189
DO NOT DISSEMINATE
DO NOT REPRODUCE

LIST OF TABLES

LIST OF TABLES (Cont'd)

LIST OF FIGURES

LIST OF FIGURES (Cont'd)

GLOSSARY OF ACRONYMS

BP	-	Backpropagation
BPCG	-	Backpropagation with Conjugate Gradients
CCD	-	Component Classification Dictionary
CRADA	-	Collaborative Research and Development Agreement
CV	-	Control Valve
CVCS	-	Chemical and Volume Control System
ES	-	Expert System
FIS	-	Flow Instrument
LCV	-	Level Control Value
LHX	-	Letdown Heat Exchanger
NN	-	Neural Network
P&ID	-	Piping and Instrumentation Diagram
PCV	-	Pressure Control Valve
PID	-	Piping and Instrumentation Database
PRODIAG	-	Process Diagnostics
PT-CV	-	Pressure Transmitter for Control Valve
RCS	-	Reactor Coolant System
RHT	-	Residual Heat Tank
RHX	-	Regenerative Heat Exchanger
SI	-	Seal Injection
T-H	-	Thermal-Hydraulic
TE-CV	-	Temperature Element for Control Valve

GLOSSARY OF ACRONYMS (Cont'd)

TI	-	Temperature Indicator
V&V	-	Verification and Validation
VCT	-	Volume Control Tank

NOMENCLATURE

E	-	same as E_p, but summed over all pattern presentations
E_p	-	neural network error for the presentation of pattern p defined as the difference between the desired target values and network activation levels summed over all output nodes
ϵ_s	-	secondary threshold
CVXX	-	chemical and volume control system malfunction number "XX"
CVXX-YY	-	CVXX with failure extent "YY"
J_ℓ	-	total number of nodes in the *ℓ-th* layer of a multilayer neural network
$\theta_j^{(\ell)}$	-	threshold value of the *j-th* node in the *ℓ-th* layer
t_{pj}	-	target value of the *j-th* node in the output layer associated with the *p-th* teaching pattern
$w_{FE\text{-}145}$	-	mass flow rate as measured by flowmeter FE-145
$w_{FT\text{-}121}$	-	mass flow rate as measured by flowmeter FT-121
$w_{ji}^{(\ell)}$	-	weight connecting the *i-th* node in the *(ℓ-1)-th* layer with the *j-th* node in the *ℓ-th* layer of a multilayer neural network
$x_{pj}^{(\ell)}$	-	activation level of the *j-th* node in the *ℓ-th* layer associated with the *p-th* teaching pattern

TERMINOLOGY

activation level	-	numerical value of the output of a neural network node
blind test	-	test in which the identity of the transient events is not known
blind-blind test	-	test in which the identity of the transient events and the type of events that can be simulated are not known
closed loop	-	loop with the same component at the two end conditions (see **loop)**
component-level diagnosis	-	diagnosis that discriminates among the multiple components hypothesized by the plant-level diagnosis (see **plant-level diagnosis)**
externally connected system	-	thermal-hydraulic system which is hydraulically connected to another system at one location during transient conditions but is valved off during normal operation
faulty region	-	region of state-space associated with a particular set of malfunctions
feedforward multilayer neural network	-	neural network modeled with three or more layers of nodes in which the information flows from the nodes located at the first layer (input layer) to the nodes located in the output layer through a set of intermediate layers known as hidden layers
input-output teaching	-	set of pairs of numbers used to train a neural network the relationship between the input values and output values
loop	-	continuous fluid circuit of monodirectional incompressible flow between two end conditions
lower part of the faulty region	-	subregion of the faulty region located below the steady-state normal operating region
NN architecture	-	defines the arrangement of nodes in a neural network
neural network	-	mathematical processing elements composed of many compututional units or nodes arranged in patterns reminiscent of biological neural networks
node	-	most fundamental computational element of neural networks
"normal" system	-	thermal-hydraulic system which is hydraulically connected to other systems with non-zero flow during normal operation

TERMINOLOGY (Cont'd)

open loop	-	loop with two different components at the two end conditions (see **loop**)
plant-level diagnosis	-	diagnosis that, in general, hypothesizes various possible faulty component candidates
secondary system	-	thermal-hydraulic system which is thermally (but not hydraulically) coupled with another system during normal operation
segment	-	portion of a loop (see **loop**)
semi-blind test	-	test in which the identity of the transient events is known but the events were not used to verify the logic of the diagnostic system
sigmoidal activation function	-	type of nonlinear function used to model the relationship between the input and output values of a neural network node
state-space	-	space spanned by the variables that define the state of the system (in our case, flowmeters FE-145 and FT-121)
steady-state normal region	-	region of state-space associated with normal steady-state operations
upper part of the faulty region	-	subregion of the faulty region located above the steady-state normal operating region

1.0 INTRODUCTION AND SUMMARY

The purpose of this volume is to present the verification and validation (V&V) results obtained by using both the Expert System (ES) portion and Neural Network (NN) portion of the developed PRODIAG code to diagnose transient events. As discussed in Volume 1 of this report, the following simplifications were made in the development of the diagnostic systems: (1) only single component failures are to be treated, (2) the transient data are noise-free, and (3) the thermal-hydraulic (T-H) system consists of single-phase liquid plus noncondensable gas. In addition, due to the "proof-of-concept" nature of the project, no attempt was made to optimize PRODIAG in order to obtain real-time performance. Nevertheless, we expect to achieve close to real-time performance once the code is optimized and run on a faster platform.

In the following chapters we describe, in detail, the various V&V stages of the development cycle of the ES and the NNs. In summary, a total of ninety-seven transient events were used to V&V the ES. Forty-eight percent of the transients were uniquely identified, thirteen percent were identified as one of two possibilities, twenty-eight percent were identified as one of many possibilities, three percent were incorrectly identified and in eight percent of the transients no diagnosis was made. All misdiagnosed transients and twenty-five percent of the unidentified transients, i.e., two percent of the total transients, were related to instrumentation faults rather then component faults. Although the ES contains a limited number of first-principles rules for detecting signal faults, signal validation is beyond the scope of the work performed for this CRADA. Of the remaining seventy-five percent of the unidentified events, fifty percent were related to transients simulated with small severity levels that could not be detected by the ES and the remaining twenty-five percent were not detected due to the lack of fidelity in the simulator models. The lack of fidelity was detected by the ES as an inconsistency in the data set, which caused the termination of the diagnostic session.

As discussed in Volume 1, due to the lack of component-specific T-H characteristic data, the novel NN concept for diagnosis developed in this project was used to perform plant-level diagnostics instead of the original plan of using it for component-level diagnostics. Even at the plant level, characteristics data of the T-H system were not available and were backed out from

a limited number of simulated transients. Nevertheless, the data were sufficient to validate the theoretical concepts of this novel approach and to allow the training and testing of the NNs. Once trained, the NNs correctly identified the imbalance type and malfunction location for all transients used for validation.

In summary, PRODIAG is shown here as being capable of identifying unanticipated events when limited plant instrumentation is available. The diagnosis capability decreases with decreasing numbers of available instruments (as expected) and with decreasing severity of the component fault. Mild transients, with small severity levels may not be detected by the diagnostic system due to the lack of sufficient signature in the data.

The remainder of this volume is divided into three chapters:

2.0 Expert System Verification and Initial Validation
3.0 Expert System Final Validation
4.0 Neural Networks Verification and Validation

The verification of the ES and its preliminary validation is documented in Chapter 2. Section 2.1 describes the plant system used as the test bed for both the ES portion and the NN portion of PRODIAG. Section 2.2 presents the transient database used to verify the ES logic and to perform preliminary validation. Section 2.3 presents the results obtained with the developmental set of simulations of the transient test matrix and Section 2.4 shows the results of a semi-blind test where the identities of the transients were known. A summary of the results obtained in Sections 2.3 and 2.4 is presented in Section 2.5. The final validation of the ES in the form of a blind test is documented in Chapter 3. Section 3.1 presents the transient data used in the blind test and Section 3.2 shows the results. The criteria used to determine the performance of the ES are presented in Section 3.3. The overall validation results of the ES are summarized in Section 3.4, followed by proposed future work in Section 3.5.

The V&V of the NNs is documented in Chapter 4. The plant system configuration used to test the NN portion of PRODIAG is described in Section 4.1 together with a summary of the

distinctive signatures that the different malfunctions have in this configuration. Section 4.2 presents the transient data base available for testing and in Section 4.3 the verification of the component-characteristics approach to plant-level diagnostics is discussed. In Section 4.4 the NN approach chosen to implement the diagnostic system is described together with a discussion on the data preprocessing and the generation of the teaching patterns used for training the feedforward NN. Section 4.5 discusses the validation of the plant-level component-characteristics NN diagnostic system developed here followed by concluding remarks in Section 4.6.

2.0 EXPERT SYSTEM VERIFICATION AND INITIAL VALIDATION

In this chapter we present the plant system used as the test bed for PRODIAG. Also, we present the transient database used to verify the reasoning framework and knowledge base of the ES and to perform preliminary validation tests of the system. We present the validation results for 58 transient events where the identities of the transients were known before the analysis was performed.

2.1 The Chemical and Volume Control System

The Chemical and Volume Control System (CVCS) of ComEd's Braidwood pressurized water reactor was selected as the test bed for the development of the PRODIAG process diagnostics code. The CVCS was selected for the following reasons: (1) it operates continuously throughout the various states of the plant, (2) it consists of a single-phase liquid system (subcooled water) plus separated volumes containing noncondensable gas over single-phase liquid, (3) it allows for a large number of transients to be modeled by the full-scope operator training Braidwood simulator, and (4) it is relatively well, but not atypically, instrumented.

The simplified piping and instrumentation diagram (P&ID) of the CVCS for the Braidwood simulator that is used as the test bed for the diagnostic system is shown in Fig. 2.1. The simplified P&ID is very similar to the original P&ID with the exception that here we removed some lines that are either usually closed during normal operation, e.g., excess letdown line, or that are used during other modes of the system operation, e.g., boration and dilution operation.

Letdown water leaves the Reactor Coolant System (RCS), represented in the upper-left portion of the Fig. 2.1, and flows through the shell-side of the regenerative heat exchanger (RHX) where it gives up its heat to makeup water being returned to the RCS. From there, letdown water proceeds through a series of valves and the letdown heat exchanger (LHX), in order to reduce system pressure and temperature, until it reaches the Volume Control Tank (VCT). Then, the charging pump (pump A in the figure) takes the coolant from the VCT to a junction point (junction 7 in the figure), where the streams divide. Charging water flows back to the

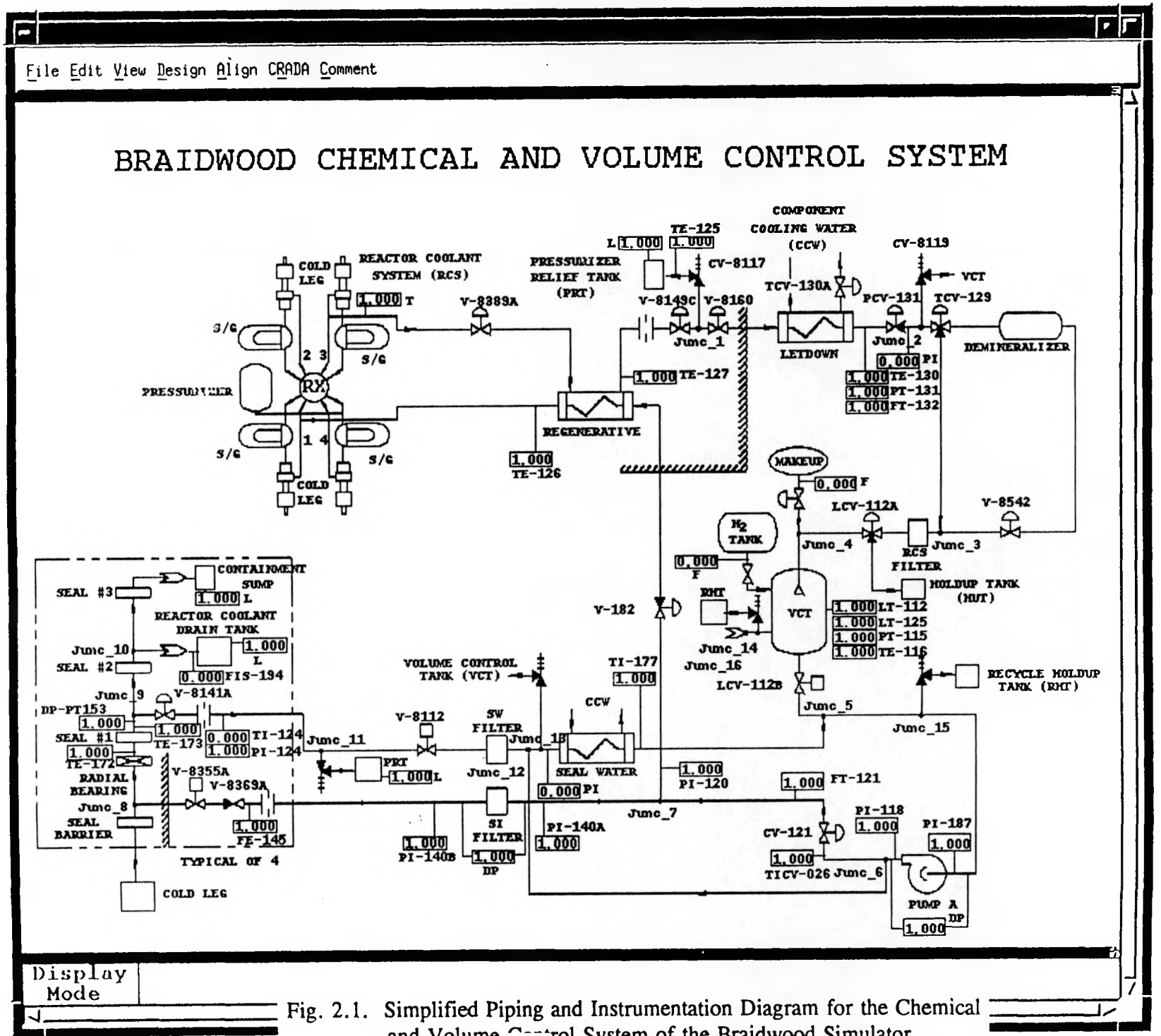

Fig. 2.1. Simplified Piping and Instrumentation Diagram for the Chemical and Volume Control System of the Braidwood Simulator

RCS through the tube-side of the RHX and the remaining water flows to the seals of the reactor coolant pumps where one portion returns to the RCS and the other recirculates.

For purposes related to the diagnostic strategy used in PRODIAG, the P&ID illustrated in Fig. 2.1 was partitioned into seventeen T-H loops as indicated in Table 2.1 ([2.1] and [2.2]). A T-H loop is defined as a sequence of components connected through piping where the process fluid flows in the same direction. As discussed in Chapter 3.0 of Volume 1, thermal-hydraulic loops can be either open or closed, and can be further classified as being a secondary system, an externally connected system, or a "normal" system [2.1]. Furthermore, each loop has a status value which indicates the type of imbalance (mass, energy, or momentum) and the trend of the imbalance (constant, increasing, or decreasing) that the loop is experiencing.

Figure 2.1 also shows the location of the 33 plant parameters that are recorded at 1 second sampling intervals for each simulation. While most of the plant parameters are located in the CVCS, some are located in other systems that are coupled with the CVCS, e.g., pressurizer, reactor cooling system, relief tanks. A color version of Fig. 2.2, where the piping between the regenerative and letdown heat exchangers is highlighted, is used as the graphical diagnostics interface between PRODIAG and the user. The graphical interface illustrates faulty components in red, increasing values of sensor measurements in green, and decreasing values of sensor measurements in yellow [2.3].

Twenty distinct CVCS transient event types that could be modeled by the full-scope Braidwood simulator were selected as the transient test matrix for V&V of PRODIAG. The description of the 20 distinct transient event types is presented in Table 2.2 and their corresponding location in the P&ID is illustrated in Fig. 2.3.

2.2 Transient Database

A total of 58 CVCS transient events separately simulated by the full-scope Braidwood simulator were used to verify the ES and perform preliminary validation. These events were obtained by simulating the 20 distinct transient event types in Table 2.2 with randomly selected severity

Table 2.1. Description of the Loops of the Chemical and Volume Control System

Loop Number	Loop Type/Complexity	Most Upstream Component	Most Downstream Component
1	open/ss[a]	cold leg 3	volume control tank (VCT)
2	opens/ss	volume control tank	cold leg 1
3	closed/ss	centrifugal pump A	centrifugal pump A
4	open/ecs[b]	junction 1	pressurizer relief tank (PRT)
8	open/ecs	junction 2	recycle holdup tank (RHT)
9	open/ns[c]	valve TCV-129	junction 3
10	open/ecs	valve LCV-112A	holdup tank (HUT)
11	open/ecs	makeup system	junction 4
12	open/ecs	hydrogen tank	volume control tank
13	open/ecs	volume control tank	recycle holdup tank
14	open/ecs	junction 15	recycle holdup tank
15	open/ns	junction 8	cold leg 4
16	open/ns	junction 9	reactor coolant drain tank (RCDT)
17	open/ns	junction 10	containment sump
18	open/ecs	junction 11	pressurizer relief tank
19	open/ns	junction 6	junction 12
20	open/ecs	junction 13	recycle holdup tank

[a]ss = secondary system
[b]ecs = externally connected system
[c]ns = "normal" system

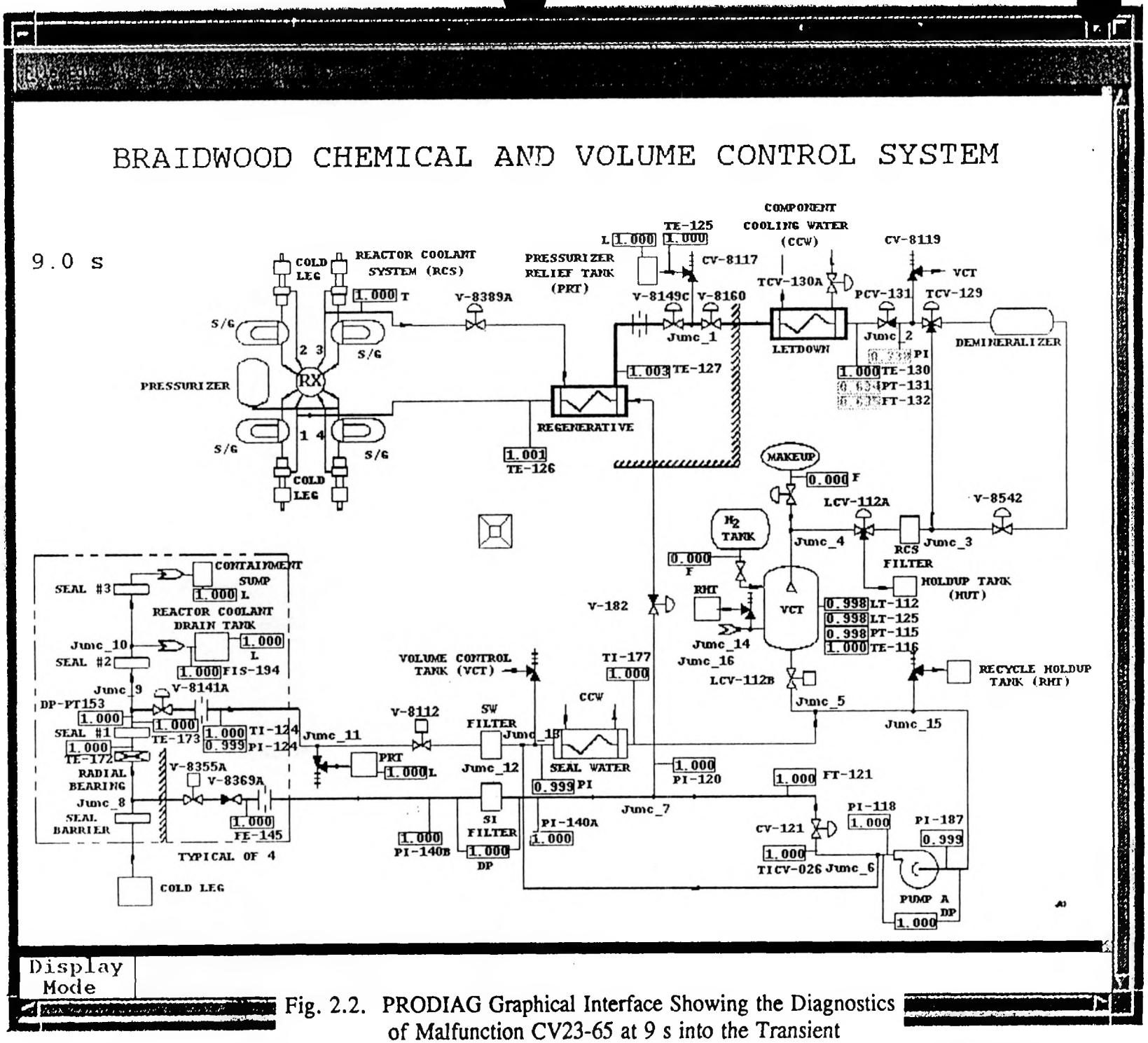

Fig. 2.2. PRODIAG Graphical Interface Showing the Diagnostics of Malfunction CV23-65 at 9 s into the Transient

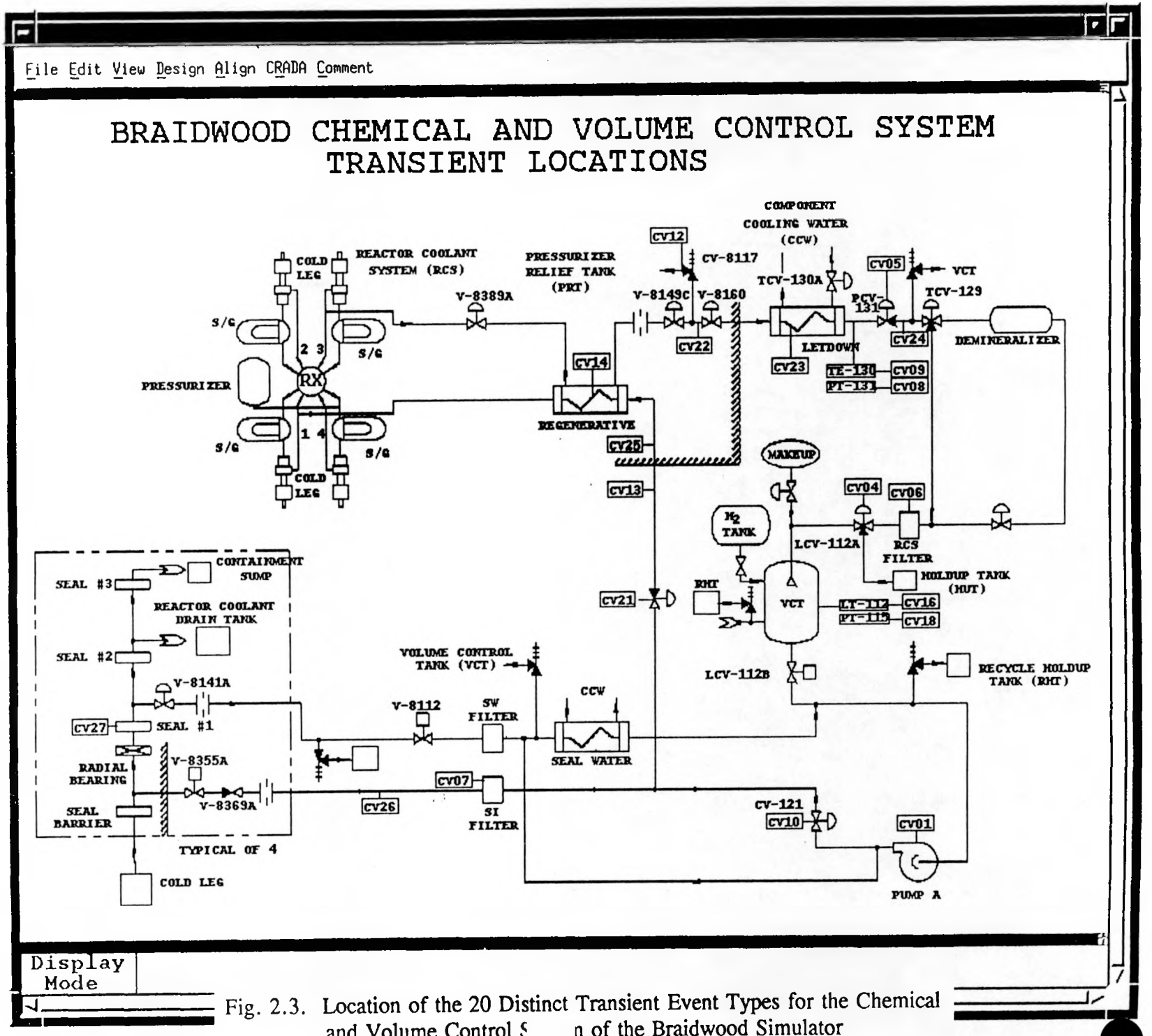

Fig. 2.3. Location of the 20 Distinct Transient Event Types for the Chemical and Volume Control S n of the Braidwood Simulator

Table 2.2. List and Description of the 20 Malfunctions

MALFUNCTION	
Type	Description
CV01	charging pump A trip
CV04	divert valve LCV-112A failure
CV05	pressure control valve PCV-131 failure
CV06	reactor coolant system (RCS) filter clogged
CV07	seal injection (SI) filter clogged
CV08	pressure transmitter PT-CV131 failure
CV09	temperature transmitter TE-CV130 failure
CV10	flow control valve CV-121 failure
CV12	letdown relief valve CV-8117 fails open
CV13	charging line leak outside containment
CV14	regenerative heat exchanger tube leak
CV16	volume control tank level malfunction
CV18	volume control tank pressure malfunction
CV21	charging header pressure control valve HCV-182 failure
CV22	letdown line leak inside containment
CV23	letdown heat exchanger tube leak
CV24	letdown line leak outside containment
CV25	charging line leak inside containment
CV26	seal injection line leak outside containment
CV27	reactor coolant pump seal #1 failure

levels for each simulation. Each single-fault transient event was simulated for 240 seconds, including at least 30 seconds of null transient, starting from a steady-state normal charging/letdown mode of the CVCS operation with the plant at 100% of nominal power. From the original files of each simulated event we selected the data from the *28-th* second through the

67-th second and constructed a new set of files consisting of only 40 seconds of data. Hence, the new data files consisted of at least 3 seconds of null transient. From now on, all time references to transient events will be made with respect to the new data files.

The 58 transients were divided into two sets containing 20 and 38 transient events, respectively. The first set was constructed such that it contained one transient of each one of the 20 distinct event types of the transient test matrix and each transient had a relatively large failure severity. The results of this set of data are presented in Section 2.3. The second set contains the remaining 38 transients, where each one of the 20 distinct event types is simulated twice with varying degrees of failure severity, with the exception of CV01 which only has one failure severity and was not represented. The results of this set of data are presented in Section 2.4.

2.3 Developmental Transient Test Matrix Results

The 20 distinct event types of the transient test matrix were used both to verify the reasoning framework and knowledge base of the ES and to perform preliminary system validation. The bulk of the ES verification was performed with these 20 transients, but it continued throughout the semi-blind test presented in the next section. The validation of the ES results, on the other hand, was an ongoing process that ended after all simulated transients were tested.

Table 2.3 shows the diagnostic results obtained with the ES for each one of the 20 transients of the first set of data of the transient test matrix as a function of time. The transient name, type, and severity, where applicable, are described in the first column of the table. The second column indicates the transient time, while the last column indicates the hypothesized faulty component candidates and comments associated with the corresponding transient time in the second column. The diagnostic information in Table 2.3 was collected from the graphical and textual interfaces provided by PRODIAG. Figure 2.2 illustrates the graphical interface for CV23-65 at 9 seconds into the transient and Fig. 2.4 illustrates the textual interface for the first 9 seconds of the transient.

Table 2.3. Expert System Diagnostic Results for the Twenty Distinct Event Types of the Transient Test Matrix

Malfunction Type - Extent	Time into the Transient (s)	Diagnosis
CV01-100 pump A trip	4	- {pump A, valve CV-121} - clogged piping between pump A and junction 7 - break between pump A and valve CV-121
	5	- {pump A, valve LCV-112B, recycle holdup tank, recycle holdup tank relief valve} - clogged piping between VCT and pump A - break between VCT and valve CV-121
	6-8	- {pump A, valve LCV-112B} - clogged piping between VCT and pump A
	9	- End of diagnostics. Pump A inlet pressure is increasing. (This pressure should have increased early on during the transient. It increased now as a secondary effect due to the increase in the VCT level and pressure).
CV04-100 valve LCV-112A fails open 100%	5	- A component is malfunctioning, however, there isn't enough information to identify the fault.
	6-7	- {valve LCV-112A, valve TCV-129, valve 8542} - break between letdown heat exchanger and VCT
	8-11	- {valve LCV-112A, valve TCV-129} - break between letdown heat exchanger and VCT
	12	- End of diagnostics. Pump A inlet pressure is decreasing. (The pressure decrease is a secondary effect due to the decrease in VCT level and pressure).
CV05-310 valve PCV-131 fails open	7-40	- {valve PCV-131}

Table 2.3. Expert System Diagnostic Results for the Twenty Distinct Event Types of the Transient Test Matrix (Cont'd)

Malfunction Type - Extent	Time into the Transient (s)	Diagnosis
CV06-100 RCS filter clogged 100%	4-6	- {RCS filter, valve TCV-129, demineralizer, valve 8542, valve LCV-112A} - clogged piping between valve PCV-131 and VCT
	7	- End of diagnostics. Letdown heat exchanger outlet flow attains nonmonotonic behavior; first it decreased and now it is increasing. (This nonmonotonic behavior is due to automatic control actions that opened relief valve CV-8119 on high PT-131 pressure).
CV07-100 SI filter clogged 100%	4-40	- {SI filter}
CV08-480 pressure transmitter PT-CV131 fails high	4-40	- {valve 8389A, valve 8149C, valve 8160}
CV09-150 temperature transmitter TE-CV131 fails high	4	- {letdown heat exchanger}. End of diagnostics.
CV10-100 flow control valve CV-121 fails open	4	- {valve CV-121, pump A}
	5-13	- {valve CV-121}
	14	- End of diagnostics. Pump A inlet pressure is decreasing. (The pressure decrease is a secondary effect due to the decrease in VCT level and pressure).

Table 2.3. Expert System Diagnostic Results for the Twenty Distinct Event Types of the Transient Test Matrix (Cont'd)

Malfunction Type - Extent	Time into the Transient (s)	Diagnosis
CV12-65 letdown relief valve CV-8117 fails open	4-9	- {valve CV-8117, pressurizer relief tank, valve 8389A, valve 8149C, valve 8160} - break between cold leg 3 and letdown heat exchanger - clogged piping between cold leg 3 and letdown heat exchanger
	10-31	- {valve CV-8117, pressurizer relief tank} - break between regenerative heat exchanger and letdown heat exchanger
	32	- End of diagnostics. Pump A inlet pressure is decreasing. (The pressure decrease is a secondary effect due to the decrease in VCT level and pressure).
CV13-45 charging line leak outside containment	4-5	- {valve HCV-182} - break between junction 7 and cold leg 1 - break between valve CV-121 and SI filter
	6-19	- break between junction 7 and regenerative heat exchanger - break between valve CV-121 and SI filter
	20	- End of diagnostics. Letdown heat exchanger outlet flow and pressure change due to automatic control actions.
CV14-65 regenerative heat exchanger tube leak	5	- A component is malfunctioning, however, there is not enough information to identify the fault.
	6	- regenerative heat exchanger tube leak. End of diagnostics.
CV16-95 VCT level fails high	5	- Instrumentation error was detected in the VCT. End of diagnostics.
CV18-70 VCT pressure fails high	5	- Instrumentation error was detected in the VCT. End of diagnostics.

Table 2.3. Expert System Diagnostic Results for the Twenty Distinct Event Types of the Transient Test Matrix (Cont'd)

Malfunction Type - Extent	Time into the Transient (s)	Diagnosis
CV21-50 pressure control valve HCV-182 fails open	4	- A component is malfunctioning, however, there is not enough information to identify the fault.
	5-7	- {valve HCV-182} - clogged piping between junction 7 and cold leg 1 - break between valve CV-121 and cold leg 1 - break between valve CV-121 and SI filter
	8-33	- {valve HCV-182} - clogged piping between junction 7 and cold leg 1 - break between regenerative heat exchanger and cold leg 1
	34	- End of diagnostics. Valve HCV-182 inlet pressure is decreasing. (This pressure should have decreased early on during the transient).
CV22-65 letdown leak inside containment	4-7	- {valve 8389A, valve 8149C, valve 8160} - clogged piping between cold leg 3 and letdown heat exchanger - break between cold leg 3 and letdown heat exchanger
	8-18	- break between regenerative heat exchanger and letdown heat exchanger
	19	- End of diagnostics. Pump A inlet pressure is decreasing. (The pressure decrease is a secondary effect due to the decrease in VCT level and pressure).
CV23-65 letdown heat exchanger tube leak	5-8	- {valve 8389A, valve 8149C, valve 8160} - clogged piping between cold leg 3 and letdown heat exchanger - break between cold leg 3 and letdown heat exchanger
	9-21	- break between regenerative heat exchanger and letdown heat exchanger
	22	- End of diagnostics. Pump A inlet pressure is decreasing. (The pressure decrease is a secondary effect due to the decrease in VCT level and pressure).

Table 2.3. Expert System Diagnostic Results for the Twenty Distinct Event Types of the Transient Test Matrix (Cont'd)

Malfunction Type - Extent	Time into the Transient (s)	Diagnosis
CV24-65 letdown line leak outside containment	5-8	- {valve TCV-129, valve 8542, valve LCV-112A} - break between letdown heat exchanger and VCT
	9-13	- {valve TCV-129, valve LCV-112A} - break between letdown heat exchanger and VCT
	14	- End of diagnostics. Pump A inlet pressure is decreasing. (The pressure decrease is a secondary effect due to the decrease in VCT level and pressure).
CV25-45 charging line leak inside containment	4	- {valve HCV-182} - clogged piping between junction 7 and cold leg 1 - break between junction 7 and cold leg 1 - break between valve CV-121 and SI filter
	5-14	- break between junction 7 and regenerative heat exchanger - break between valve CV-121 and SI filter
	15	- End of diagnostics. Letdown heat exchanger outlet pressure changes due to automatic control actions.
CV26-20 seal injection line leak outside containment	4-40	- break between SI filter and valve 8369A
CV27-150 seal #1 leakoff flow increase	4	- {seal #1, pump A, valve CV-121, SI filter, valve 8369A, valve 8355A, valve 8141A, valve 8112, SW filter} - clogged piping between junction 9 and seal #2 - clogged piping between pump A and pump A
	5	- {seal #1, valve 8369A, valve 8355A, valve 8141A}
	6	- End of diagnostics. Seal #1 radial bearing outlet temperature attains a nonmonotonic behavior. (Due to reverse flow).

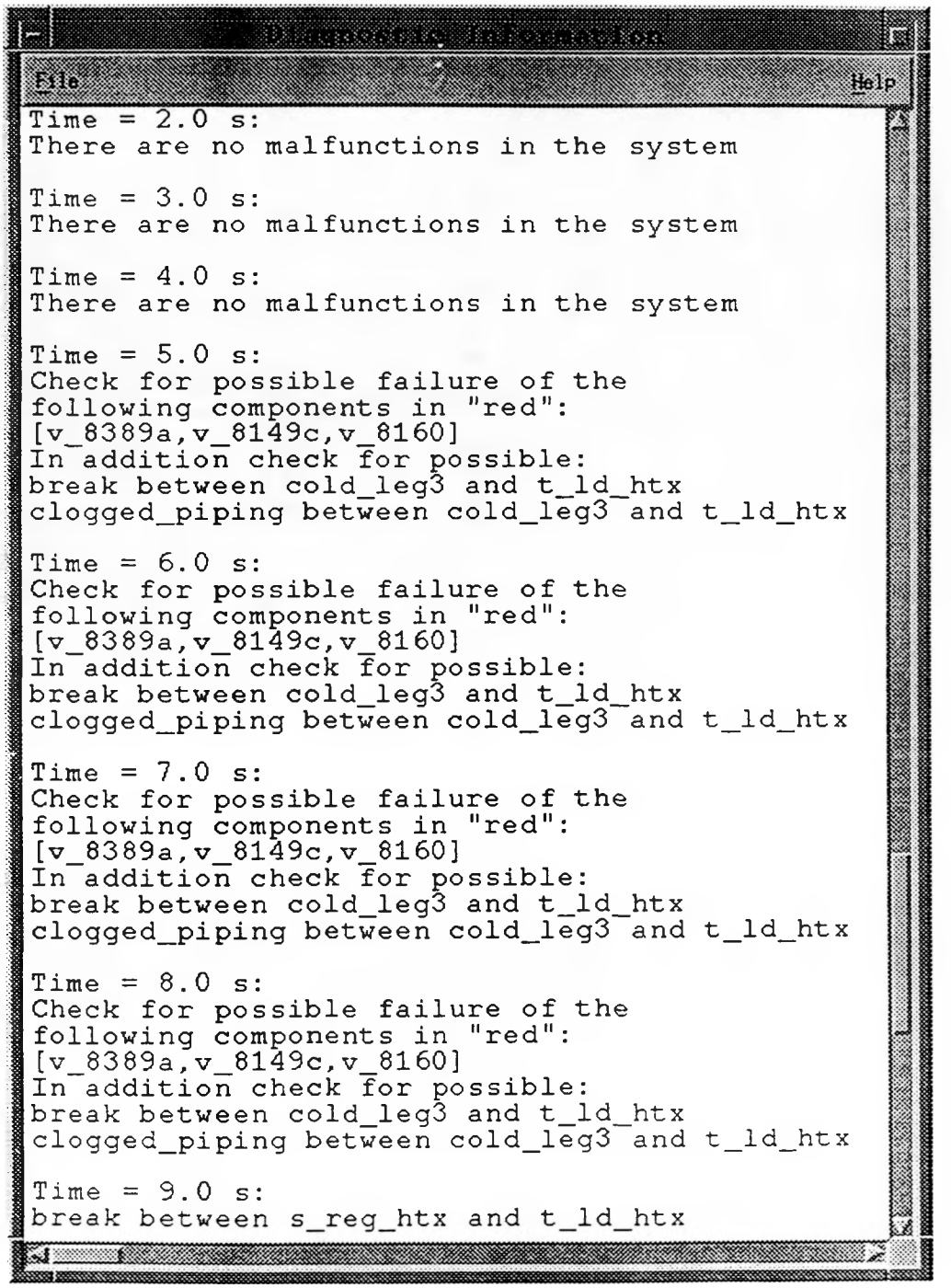

Fig. 2.4. PRODIAG Textual Interface Showing the Diagnostics of Malfunction CV23-65 at the First 9 Seconds into the Transient

Table 2.4 summarizes the diagnostic results for the 20 events in Table 2.3. Since nuclear power plant transients are dynamic phenomena that evolve in time, so do the diagnostics. Therefore, in the summary of the diagnostic results in Table 2.4 we present the inference performed at the end of the 40-second diagnostic period. In cases where the diagnostics were halted before 40 seconds, the results correspond to the last second before the diagnostics were halted. The five columns of Table 2.4 illustrate if the transient is uniquely identified, identified as one of two possibilities, identified as one of many possibilities, incorrectly identified, or not identified, respectively, along with the corresponding transients.

Table 2.4. Summary of the Expert System Results for the 20 Distinct Event Types of the Transient Test Matrix

Uniquely Identified	Identified as One of Two Possibilities	Identified as One of Many Possibilities	Incorrect Diagnostics	No Diagnostics
10 (50%)	2 (10%)	7 (35%)	1 (5%)	–
CV05-310	CV13-45	CV01-100	CV08-480	
CV07-100	CV25-45	CV04-100		
CV09-150[a]		CV06-100		
CV10-100		CV12-65		
CV14-65		CV21-50		
CV16-95		CV24-65		
CV18-70		CV27-150		
CV22-65				
CV23-65				
CV26-20				

[a]A sensor associated with the identified component is the root cause

Ten transients, corresponding to 50% of the transients in the first set, are uniquely identified, 2 transients or 10% are identified as one out of two possibilities, 7 transients or 35% are identified as one out of many, and 1 or 5% is incorrectly identified. The incorrectly identified transient, CV08, corresponds to a pressure transmitter failure which causes the instantaneous

action of the CVCS automatic control system, which in turn, actuates a valve causing other sensors to deviate from their expected values. The fact that CV08 is an instrumentation error coupled with the instantaneous control action prevents the detection of this transient type. The ES was designed primarily to detect component malfunctions, and not to perform signal validation.

2.4 Semi-Blind Test Results

With the bulk of the reasoning framework and knowledge base of the ES verified, the second set of transient data discussed in Section 2.2 was used to further validate the system through a semi-blind test.

Table 2.5 shows the diagnostic results obtained with the ES for each one of the 38 transients of the semi-blind test as a function of time. The transient name, type, and severity (where applicable) are described in the first column of the table. The second column indicates the transient time, while the last column indicates the hypothesized faulty component candidates and comments associated with the corresponding transient time in the second column. For this set of data, transients in which none of the sensors reached the diagnostics initiating threshold [2.4] (due to small fault severity) within the first 40 seconds are tested for 120 seconds.

Similar to Table 2.4, in Table 2.6 we summarize the diagnostic results for the 38 events of Table 2.5. Seventeen transients, corresponding to 45% of the transients in the second set, are uniquely identified, 8 transients or 21% are identified as one out of two possibilities, 5 transients or 13% are identified as one out of many, 2 or 5% are incorrectly identified, and 6 or 16% are not identified. As in the first set of 20 transients, CV08 is once again incorrectly diagnosed. However, unlike the first set of transients, in this set 6 transients are not identified. Four out of the 6 unidentified transients, CV04-10, CV04-50, CV06-10, and CV24-10, are not diagnosed due to their small failure severity. Small severity values preclude the sensors from reaching the threshold [2.4] used to indicate that the sensor is deviating from its expected value and, hence, decrease the information available for diagnostics. The other two unidentified transients, CV21-10 and CV21-100, are not identified due to inaccuracies (or lack of fidelity) in the simulation data. The lack of fidelity causes the pressure across the seal injection (SI) filter to incorrectly change trends in two consecutive time steps (see table 2.5 and reference [2.5]).

Table 2.5. Expert System Results for the 38 Transient Events of the Semi-Blind Test

Malfunction Type - Extent	Time into the Transient (s)	Diagnosis
CV04-10 valve LCV-112A fails open 10%	1-120	- No diagnostics. None of the measured variables reached the threshold in 120s.
CV04-50 valve LCV-112A fails open 50%	5-13	- A component is malfunctioning, however, there is not enough information to identify the fault.
	14	- End of diagnostics. Pump A inlet pressure is decreasing. (The pressure decrease is a secondary effect due to the decrease in VCT level and pressure).
CV05-390 valve PCV-131 fails closed	18-40	- {valve PCV-131} - clogged piping between letdown heat exchanger and valve PCV-131
CV05-480 valve PCV-131 fails closed	5-40	- {valve PCV-131} - clogged piping between letdown heat exchanger and valve PCV-131
CV06-10 RCS filter clogged 10%	5-40	- A component is malfunctioning, however, there is not enough information to identify the fault.
CV06-50 RCS filter clogged 50%	4-40	- {RCS filter, valve TCV-129, demineralizer, valve 8542, valve LCV-112A} - clogged piping between valve PCV-131 and VCT
CV07-10 SI filter clogged 10%	4-5	- A component is malfunctioning, however, there is not enough information to identify the fault.
	6	- Instrumentation error was detected in the SI filter. (This is due to the approximations in the simulation models which yield an increase in the pressure difference across the filter with the downstream flow decreasing and a constant upstream flow). End of diagnostics.
CV07-50 SI filter clogged 50%	4	- {SI filter, pump A, valve CV-121} - clogged piping between pump A and SI filter - break between pump A and valve CV-121
	5-40	- {SI filter}

Table 2.5. Expert System Results for the 38 Transient Events of the Semi-Blind Test (Cont'd)

Malfunction Type - Extent	Time into the Transient (s)	Diagnosis
CV08-310 pressure transmitter PT-CV131 fails low	4-10	- {valve 8389A, valve 8149C, valve 8160} - clogged piping between cold leg 3 and letdown heat exchanger - break between cold leg 3 and letdown heat exchanger
	11-40	- {valve 8389A, valve 8149C, valve 8160} - clogged piping between cold leg 3 and letdown heat exchanger - break between cold leg 3 and regenerative heat exchanger
CV08-390 pressure transmitter PT-CV131 fails high	5	- A component is malfunctioning, however, there is not enough instrumentation to identify the fault.
	6-7	- {valve 8389A, valve 8149C, valve 8160}
	8	- End of diagnostics. Valve PT-CV131 outlet pressure increases as the result of control actions.
CV09-130 temperature transmitter TE-CV131 fails high	4	- {letdown heat exchanger}. End of diagnostics.
CV09-70 temperature transmitter TE-CV131 fails low	4	- {letdown heat exchanger}. End of Diagnostics.
CV10-10 flow control valve CV-121 fails closed	4	- A component is malfunctioning, however, there is not enough information to identify the fault.
	5-19	- {valve CV-121} - clogged piping between junction 6 and junction 7
	20	- End of diagnostics. Pump A inlet pressure is increasing. (The pressure increase is a secondary effect due to the increase in VCT level and pressure).

Table 2.5. Expert System Results for the 38 Transient Events of the Semi-Blind Test (Cont'd)

Malfunction Type - Extent	Time into the Transient (s)	Diagnosis
CV10-50 flow control valve CV-121 fails open	4-16	- {valve CV-121}
	17	- End of diagnostics. Pump A inlet pressure is decreasing. (The pressure decrease is a secondary effect due to the decrease in VCT level and pressure).
CV12-10 letdown relief valve CV-8117 fails open	4-40	- {valve CV-8117, pressurizer relief tank, valve 8389A, valve 8149C, valve 8160} - clogged piping between cold leg 3 and letdown heat exchanger - break between cold leg 3 and letdown heat exchanger
CV12-35 letdown relief valve CV-8117 fails open	4-12	- {valve CV-8117, pressurizer relief tank, valve 8389A, valve 8149C, valve 8160} - clogged piping between cold leg 3 and letdown heat exchanger - break between cold leg 3 and letdown heat exchanger
	13-40	- {valve CV-8117, pressurizer relief tank} - break between regenerative heat exchanger and letdown heat exchanger
CV13-10 charging line leak outside containment	4-5	- {valve HCV-182} - break between junction 7 and cold leg 1 - break between valve CV-121 and SI filter
	6-40	- break between junction 7 and regenerative heat exchanger - break between valve CV-121 and SI filter
CV13-25 charging line leak outside containment	4-5	- {valve HCV-182} - break between junction 7 and cold leg 1 - break between valve CV-121 and SI filter
	6-40	- break between junction 7 and regenerative heat exchanger - break between valve CV-121 and SI filter
CV14-10 regenerative heat exchanger tube leak	9	- A component is malfunctioning, however, there is not enough information to identify the fault.
	10	- regenerative heat exchanger tube leak. End of diagnostics.

Table 2.5. Expert System Results for the 38 Transient Events of the Semi-Blind Test (Cont'd)

Malfunction Type - Extent	Time into the Transient (s)	Diagnosis
CV14-35 regenerative heat exchanger tube leak	6	- regenerative heat exchanger tube leak. End of diagnostics.
CV16-15 VCT level fails low	4	- A component is malfunctioning, however, there is not enough information to identify the fault.
	5	- Instrumentation error was detected in the VCT. End of diagnostics.
CV16-75 VCT level fails high	4	- A component is malfunctioning, however, there is not enough information to identify the fault.
	5	- Instrumentation error was detected in the VCT. End of diagnostics.
CV18-05 VCT pressure fails low	4	- A component is malfunctioning, however, there is not enough information to identify the fault.
	5	- Instrumentation error was detected in the VCT. End of diagnostics.
CV18-20 VCT pressure fails low	4	- A component is malfunctioning, however, there is not enough information to identify the fault.
	5	- Instrumentation error was detected in the VCT. End of diagnostics.
CV21-10 pressure control valve HCV-182 fails closed	3	- {pump A, valve 8369A, valve 8355A, seal #1, valve 8141A, valve 8112, SW filter} - clogged piping between SI filter and pump A
	4	- End of diagnostics. Pressure drop across the SI filter attains a nonmonotonic behavior. (It erroneously decreases at 3s and then increases at 4s - the problem is due to a lack of accuracy of the simulation models).

Table 2.5. Expert System Results for the 38 Transient Events of the Semi-Blind Test (Cont'd)

Malfunction Type - Extent	Time into the Transient (s)	Diagnosis
CV21-100 pressure control valve HCV-182 fails open	4	- {pump A, valve 8369A, valve 8355A, seal #1, valve 8141A, valve 8112, RHT, RHT relief valve, seal water heat exchanger relief valve} - break between SI filter and pump A
	5	- End of diagnostics. Pressure drop across the SI filter attains a nonmonotonic behavior. (It erroneously decreases at 4s and then increases at 5s - the problem is due to a lack of accuracy of the simulation models).
CV22-10 letdown leak inside containment	5-14	- {valve 8389A, valve 8149C, valve 8160} - clogged piping between cold leg 3 and letdown heat exchanger - break between cold leg 3 and letdown heat exchanger
	15-40	- break between regenerative heat exchanger and letdown heat exchanger
CV22-35 letdown leak inside containment	4-8	- {valve 8389A, valve 8149C, valve 8160} - clogged piping between cold leg 3 and letdown heat exchanger - break between cold leg 3 and letdown heat exchanger
	9-25	- break between regenerative heat exchanger and letdown heat exchanger
	26	- End of diagnostics. Pump A inlet pressure is decreasing. (The pressure decrease is a secondary effect due to the decrease in VCT level and pressure).
CV23-10 letdown heat exchanger tube leak	5-16	- {valve 8389A, valve 8149C, valve 8160} - clogged piping between cold leg 3 and letdown heat exchanger - break between cold leg 3 and letdown heat exchanger
	17-40	- break between regenerative heat exchanger and letdown heat exchanger

Table 2.5. Expert System Results for the 38 Transient Events of the Semi-Blind Test (Cont'd)

Malfunction Type - Extent	Time into the Transient (s)	Diagnosis
CV23-35 letdown heat exchanger tube leak	4-8	- {valve 8389A, valve 8149C, valve 8160} - clogged piping between cold leg 3 and letdown heat exchanger - break between cold leg 3 and letdown heat exchanger
	9-28	- break between regenerative heat exchanger and letdown heat exchanger
	29	- End of diagnostics. Pump A inlet pressure is decreasing. (The pressure decrease is a secondary effect due to the decrease in VCT level and pressure).
CV24-10 letdown line leak outside containment	5-40	- A component is malfunctioning, however, there is not enough information to identify the fault.
CV24-35 letdown line leak outside containment	4-10	- {valve TCV-129, valve 8542, valve LCV-112A} - break between letdown heat exchanger and VCT
	11-18	- {valve TCV-129, valve LCV-112A} - break between letdown heat exchanger and VCT
	19	- End of diagnostics. Pump A inlet pressure is decreasing. (The pressure decrease is a secondary effect due to the decrease in VCT level and pressure).
CV25-10 charging line leak inside containment	10-11	- {valve HCV-182} - clogged piping between junction 7 and cold leg 1 - break between valve CV-121 and cold leg 1 - break between valve CV-121 and SI filter
	12-40	- break between valve CV-121 and regenerative heat exchanger - break between junction 7 and SI filter

Table 2.5. Expert System Results for the 38 Transient Events of the Semi-Blind Test (Cont'd)

Malfunction Type - Extent	Time into the Transient (s)	Diagnosis
CV25-25 charging line leak inside containment	4	- {valve HCV-182} - clogged piping between junction 7 and cold leg 1 - break between valve CV-121 and cold leg 1 - break between valve CV-121 and SI filter
	5-40	- break between valve CV-121 and regenerative heat exchanger - break between junction 7 and SI filter
CV26-04 seal injection line leak outside containment	4	- A component is malfunctioning, however, there is not enough information to identify the fault.
	5-40	- break between SI filter and valve 8369A
CV26-10 seal injection line leak outside containment	4	- A component is malfunctioning, however, there is not enough information to identify the fault.
	5-40	- break between SI filter and valve 8369A
CV27-05 seal #1 leak off flow increase	4-5	- {seal #1, pump A, valve CV-121, valve 8369A, valve 8355A, valve 8141A}
	6	- Instrumentation error was detected in the SI filter. (This is due to the approximations in the models which yield an increase in the pressure drop across the filter with the downstream flow increasing and a constant upstream flow). End of diagnostics.
CV27-50 seal #1 leak off flow increase	4-5	- {seal #1, valve 8369A, valve 8355A, valve 8141A)
	6	- End of diagnostics. Seal #1 radial bearing outlet temperature attains a nonmonotonic behavior. (Due to reverse flow).

Table 2.6. Summary of the Expert System Results for the 38 Transient Events of the Semi-Blind Test

Uniquely Identified	Identified as One of Two Possibilities	Identified as One of Many Possibilities	Incorrect Diagnostics	No Diagnostics
17 (45%)	8 (21%)	5 (13%)	2 (5%)	6 (16%)
CV07-10[c]	CV05-390	CV06-50	CV08-310	CV04-10[a]
CV07-50	CV05-480	CV12-10	CV08-390	CV04-50[b]
CV09-130[d]	CV10-10	CV24-35		CV06-10[b]
CV09-70[d]	CV12-35	CV27-05		CV21-10[e]
CV10-50	CV13-10	CV27-50		CV21-100[e]
CV14-10	CV13-25			CV24-10[b]
CV14-35	CV25-10			
CV16-15	CV25-25			
CV16-75				
CV18-05				
CV18-20				
CV22-10				
CV22-35				
CV23-10				
CV23-35				
CV26-04				
CV26-10				

[a]None of the sensors reached the transient initiation threshold
[b]Sensors reached threshold but there wasn't enough information
[c]Instrumentation error was detected associated with faulty component
[d]A sensor associated with the identified component is the root cause
[e]Error in simulated data

2.5 Overall Preliminary Results

For the 58 transients of Sections 2.3 and 2.4, the ES correctly diagnosed 85% (49/58) of the events within the first 40 seconds into the transient, incorrectly diagnosed 5% (3/58) of the events, and did not diagnose 10% (6/58) of the events. All incorrectly diagnosed events correspond to the same event type, i.e., CV08, and the unidentified events are either transients with small fault severity or transients with inaccurate simulation data.

REFERENCES

2.1 T. Y. C. Wei, "Reasoning Algorithm Framework for Combined Expert System/Neural Network for Process Fault Diagnosis," Memorandum to J. Reifman, 20 February 1993.

2.2 J. Reifman, "Description of the Prolog Program that Generates the Knowledge Base for the Representation of the P&ID," Memorandum to T. Y. C. Wei, 11 June 1993.

2.3 G. Graham and J. Reifman, "The Display PRODIAG Interface and Results for 20 CVCS Transients," Memorandum to T. Y. C. Wei, 4 August 1994.

2.4 J. Reifman, "Incorporation of the Time-Window Selector in PRODIAG," Memorandum to T. Y. C. Wei, 26 January 1994.

2.5 Unpublished notes that present the trend of the plant parameters at every time step for each one of the simulated events (1994 and 1995).

3.0 EXPERT SYSTEM FINAL VALIDATION

The purpose of this chapter is to present the results of a blind test [3.1] for the ES portion of PRODIAG. The blind test consists of applying the developed diagnostic system to determine the identity of 42 transient events simulated by ComEd personnel. The identities of the transients were not disclosed to us until after we provided ComEd with the results obtained by the ES. We did know, however, that each one of the simulated transients represented one of 20 distinct transient types of the transient test matrix for the Braidwood CVCS. We just did not know which one. Here, we compare the faulty components hypothesized by the ES with the actual simulated fault and assess the performance of the developed diagnostic system. In addition, we summarize the validation results of the ES for all simulated transients and propose directions of future work.

3.1 Transient Database

The same P&ID of the Braidwood CVCS used for the preliminary testing of the diagnostic system discussed in the previous chapter was used to perform the blind test of the system (see Fig. 2.1). Figure 2.1 also shows the location of the 33 plant parameters that were recorded at 1 second sampling intervals for each simulation. However, during the data collection for the blind test, an incorrect interface program was used. It did not record the values of four plant parameters: pressure indicator downstream of valve PCV-131, flow indicator FIS-194 upstream of the reactor coolant drain tank, temperature indicator TI-124 downstream of valve 8141A, and pressure indicator upstream of the seal water heat exchanger. In the blind test data, the values of these four parameters were zero and could not be used for diagnostics.

Out of the four missing plant parameters, only the pressure indicator downstream of the letdown valve PCV-131 is really important in diagnosing the transient events. The missing pressure information prevents the diagnostic ES from distinguishing any transient that requires the information of this parameter with the same precision obtained in the tests presented in Chapter 2.0.

This unfortunate occurrence does, however, serve to illustrate one of the key advantages of the proposed novel diagnostic ES. The diagnostic strategy is independent of the physical process, i.e., the P&ID. Hence, there was no need to modify the first-principles rules or the logic of the diagnostic system to account for the missing instrumentation. The missing instruments only affect the precision of the diagnostics, not the reasoning algorithm. That is because, in general, the smaller the number of available instruments, the less precise is the diagnostic. This is in contrast with conventional diagnostic ESs that directly map instrumentation values into component faults, in which case the missing instrumentation would preclude performing the diagnostics.

A total of 42 CVCS transient events separately simulated by the full-scope Braidwood simulator representing 20 distinct event types were used for the blind test. These 20 event types represent the same transients described in Chapter 2.0 and presented in Table 2.2. Here, however, an additional transient event, CV29 corresponding to a charging pump A degraded impeller fault, was also simulated. This additional transient corresponds to the same event type as CV01, i.e., pump A failure, and was added to increase the testing database with a larger number of severity levels for the pump.

The 42 single-fault transients were simulated by ComEd personnel. They randomly selected event types from Table 2.2, including transient CV29, and simulated them with arbitrary failure severity. The identity of the transients were not disclosed to us until after we provided ComEd personnel with ES diagnostic results. Each single-fault transient event was simulated for 180 seconds, including at least 30 seconds of null transient, starting from a steady-state normal charging/letdown mode of the CVCS operation with the plant at 100% of nominal power. From the original files of each simulated event we selected the data from the *28-th* second through the *67-th* second and constructed a new set of files consisting of only 40 seconds of data. Hence, the new data files consisted of at least 3 seconds of null transient. From now on, all time references to transient events will be made with respect to the new data files. This is the exact same approach used in Chapter 2.0.

3.2 Blind Test Results

Table 3.1 shows the diagnostic results obtained with the ES for each one of the 42 transients of the blind test as a function of time. The filename, e.g., argonne1, argonne2, argonne3, and the associated hypothesized transient event types, e.g., CV04 or CV05 or CV06, are presented in the first column of the table. The second column indicates the transient time, while the last column presents the ES hypothesized faulty component candidates and comments associated with the corresponding transient time in the second column.

The hypothesized transient event types in the first column of the Table 3.1 were obtained by matching the hypothesized component candidates in the last column of the table with the list of possible transient types in Table 2.2. Since nuclear power plant transients are dynamic phenomena that evolve in time, so do the diagnostics. Therefore, in the hypothesized transient event types in the first column of the Table 3.1 we present the inference obtained at the end of the 40-second diagnostic period. In the case where the diagnostics were halted before 40 seconds, we present the diagnostics at the last second before the diagnostics were halted.

Table 3.2 summarizes the ES diagnostic results for each one of the 42 events in Table 3.1, and identifies the actual simulated event type and failure severity of the 42 transients. In all but five transients, argonne2, argonne7, argonne21, argonne34, and argonne44, the actual simulated transient type presented in the last column of Table 3.2 is included in the list of transient types hypothesized by the expert system and presented in the second column of the table.

These five transients correspond to two event types, CV04 and CV08. As discussed in Chpater 2.0, CV08, which corresponds to a pressure transmitter failure, i.e., a sensor failure, can not be correctly identified. The diagnostic system either incorrectly classifies CV08, or makes no inference about the transient depending on the response time of the CVCS automatic control actions. In the two simulations of CV08, argonne21 and argonne34, no diagnosis is made. Note that the first-principles ES was designed primarily to detect component malfunctions, and not to perform signal validation.

Table 3.1. Expert System Diagnostic Results for the Blind Test of the CVCS

Filename and (Transient Type)	Time into the Transient (s)	Diagnosis
argonne1 (CV04 or CV05 or CV06)	4-7	- {valve PCV-131, valve TCV-129, demineralizer, valve 8542, RCS filter, valve LCV-112A} - clogged piping between letdown heat exchanger and VCT
	8	- End of diagnostics. Letdown heat exchanger outlet flow attains nonmonotonic behavior; first it decreased and now it is increasing. (This nonmonotonic behavior is due to automatic control actions that opened relief valve CV-8119 on high PT-131 pressure).
argonne2	1-80	- No diagnostics. None of the measured variables reached the threshold in 80s.
argonne3 (CV01 ≡ CV29)	4-15	- {pump A}
	16	- End of diagnostics. Automatic control actions caused the letdown heat exchanger outlet pressure and flow to vary.
argonne4 (CV10)	5-19	- {valve CV-121} - clogged piping between junction 6 and junction 7
	20	- End of diagnostics. Seal #1 modulation caused an increase in the pressure difference across the seal.
argonne5 (CV04 or CV24)	5-6	- {valve PCV-131, valve TCV-129, valve 8542, valve LCV-112A} - break between letdown heat exchanger and VCT
	7-9	- {valve TCV-129, valve LCV-112A} - break between letdown heat exchanger and VCT
	10	- End of diagnostics. Pump A inlet pressure is decreasing. (The pressure decrease is a secondary effect due to the decrease in VCT level and pressure).

Table 3.1. Expert System Diagnostic Results for the Blind Test of the CVCS (Cont'd)

Filename and (Transient Type)	Time into the Transient (s)	Diagnosis
argonne6 (CV12 or CV14 or CV22 or CV23)	4	- A component is malfunctioning, however, there isn't enough information to identify the fault.
	5-8	- {valve 8389A, valve 8149C, valve 8160, valve CV-8117, pressurizer relief tank} - break between cold leg 3 and letdown heat exchanger - clogged piping between cold leg 3 and letdown heat exchanger
	9-21	- {valve CV-8117, pressurizer relief tank} - break between regenerative heat exchanger and letdown heat exchanger
	22	- End of diagnostics. Pump A inlet pressure is decreasing. (The pressure decrease is a secondary effect due to the decrease in VCT level and pressure).
argonne7	1-80	- No diagnostics. None of the measured variables reached the threshold in 80s.
argonne8 (CV16)	4	- A component is malfunctioning, however, there isn't enough information to identify the fault.
	5	- Instrumentation error was detected in VCT. End of diagnostics.
argonne9 (CV26)	4-36	- Break between SI filter and valve 8369A
	37	- End of diagnostics. Pump A inlet pressure is decreasing. (The pressure decrease is a secondary effect due to the decrease in VCT level and pressure).
argonne10 (CV01 = CV29)	4	- {pump A, valve CV-121} - break between pump A and valve CV-121 - clogged piping between pump A and junction 7
	5-14	- {pump A}
	15	- End of diagnostics. Automatic control actions caused the letdown heat exchanger pressure and flow to vary.

Table 3.1. Expert System Diagnostic Results for the Blind Test of the CVCS (Cont'd)

Filename and (Transient Type)	Time into the Transient (s)	Diagnosis
argonne11 (CV14 or CV22 or CV23)	4-6	- {valve 8389A, valve 8149C, valve 8160} - break between cold leg 3 and letdown heat exchanger - clogged piping between cold let 3 and letdown heat exchanger
	7-13	- break between regenerative heat exchanger and letdown heat exchanger
	14	- End of diagnostics. Pump A inlet pressure is decreasing. (The pressure decrease is a secondary effect due to the decrease in VCT level and pressure).
argonne12 (CV13 or CV21 or CV25)	4-5	- {valve HCV-182} - break between junction 7 and cold leg 1 - break between valve CV-121 and SI filter
	6-7	- break between junction 7 and regenerative heat exchanger - break between valve CV-121 and SI filter
	8-12	- {valve HCV-182} - break between junction 7 and cold leg 1 - break between valve CV-121 and SI filter
	13	- End of diagnostics. Valve 8141A outlet pressure is decreasing.
argonne13 (CV13 or CV21 or CV25)	4-7	- {valve HCV-182} - break between junction 7 and cold leg 1 - break between valve CV-121 and SI filter
	8	- End of diagnostics. Seal #1 modulation caused a decrease in the pressure difference across the seal.
argonne14 (CV07)	3	- {pump A, valve CV-121, SI filter} - break between pump A and valve CV-121 - clogged piping between pump A and SI filter
	4-40	- {SI filter}

Table 3.1. Expert System Diagnostic Results for the Blind Test of the CVCS (Cont'd)

Filename and (Transient Type)	Time into the Transient (s)	Diagnosis
argonne15 (CV04 or CV24)	6-7	- {valve PCV-131, valve TCV-129, valve 8542, valve LCV-112A} - break between letdown heat exchanger and VCT
	8-13	- {valve TCV-129, valve LCV-112A} - break between letdown heat exchanger and VCT
	14	- End of diagnostics. Pump A inlet pressure is decreasing. (The pressure decrease is a secondary effect due to the decrease in VCT level and pressure).
argonne16 (CV09)	4	- {letdown heat exchanger}. End of diagnostics.
argonne17 (CV18)	4	- A component is malfunctioning, however, there isn't enough information to identify the fault.
	5	- Instrumentation error was detected in the VCT. End of diagnostics.
argonne18 (CV05 or CV06)	7-32	- {valve PCV-131, valve TCV-129, demineralizer, valve 8542, RCS filter, valve LCV-112A} - clogged piping between letdown heat exchanger and VCT
	33-40	- {valve PCV-131, demineralizer, valve 8542, RCS filter} - clogged piping between letdown heat exchanger and junction 4
argonne19 (CV27)	4-5	- {valve 8369A, valve 8355A, seal #1, valve 8141A}
	6	- End of diagnostics. Seal #1 radial bearing outlet temperature attains a nonmonotonic behavior. (Due to reverse flow).

Table 3.1. Expert System Diagnostic Results for the Blind Test of the CVCS (Cont'd)

Filename and (Transient Type)	Time into the Transient (s)	Diagnosis
argonne20 (CV14 or CV22 or CV23)	4-6	- {valve 8389A, valve 8149C, valve 8160} - break between cold leg 3 and letdown heat exchanger - clogged piping between cold leg 3 and letdown heat exchanger
	7-15	- break between regenerative heat exchanger and letdown heat exchanger
	16	- End of diagnostics. Pump A inlet pressure is decreasing. (The pressure decrease is a secondary effect due to the decrease in VCT level and pressure).
argonne21	5-7	- A component is malfunctioning, however, there isn't enough information to identify the fault.
	8	- End of diagnostics. Letdown heat exchanger outlet flow is under the influence of control action.
argonne22 (CV13 or CV21 or CV25)	4	- {valve HCV-182} - break between junction 7 and cold leg 1 - break between valve CV-121 and SI filter - clogged piping between junction 7 and cold leg 1
	5	- {valve HCV-182} - break between junction 7 and cold leg 1 - break between valve CV-121 and SI filter
	6-8	- break between junction 7 and regenerative heat exchanger - break between valve CV-121 and SI filter
	9-21	- {valve HCV-182} - break between junction 7 and cold leg 1 - break between valve CV-121 and SI filter
	22	- End of diagnostics. Pump A inlet pressure is decreasing. (The pressure increase is a secondary effect due to the decrease in VCT level and pressure).

Table 3.1. Expert System Diagnostic Results for the Blind Test of the CVCS (Cont'd)

Filename and (Transient Type)	Time into the Transient (s)	Diagnosis
argonne23 (CV14 or CV22 or CV23)	4-7	- {valve 8389A, valve 8149C, valve 8160} - break between cold leg 3 and letdown heat exchanger - clogged piping between cold leg 3 and letdown heat exchanger
	8-16	- break between regenerative heat exchanger and letdown heat exchanger
	17	- End of diagnostics. Pump A inlet pressure is decreasing. (The pressure increase is a secondary effect due to the decrease in VCT level and pressure).
argonne24 (CV21)	3	- A component is malfunctioning, however, there isn't enough information to identify the fault.
	4	- {valve HCV-182} - break between junction 7 and cold leg 1 - break between valve CV-121 and SI filter - clogged piping between junction 7 and cold leg 1
	5	- {valve HCV-182} - break between junction 7 and cold leg 1 - break between valve CV-121 and SI filter
	6-7	- {valve HCV-182} - break between regenerative heat exchanger and cold leg 1
	8	- End of diagnostics. SI filter pressure is decreasing. (This pressure should have decreased early on during the transient).
argonne25 (CV01 = CV29 or CV10 or CV27)	4-5	- {pump A, valve CV-121, valve 8369A, valve 8355A, seal #1, valve 8141A}
	6	- Instrumentation error was detected in the SI filter. (This is due to the approximations in the simulation models which yield an increase in the pressure difference across the filter with the downstream flow decreasing and a constant upstream flow). End of diagnostics.

Table 3.1. Expert System Diagnostic Results for the Blind Test of the CVCS (Cont'd)

Filename and (Transient Type)	Time into the Transient (s)	Diagnosis
argonne26 (CV04 or CV05 or CV06)	4	- {valve PCV-131, valve TCV-129, demineralizer, valve 8542, RCS filter, valve LCV-112A} - clogged piping between letdown heat exchanger and VCT
	5	- End of diagnostics. Letdown heat exchanger outlet flow attains nonmonotonic behavior; first it decreased and now it is increasing. (This nonmonotonic behavior is due to automatic control actions that opened relief valve CV-8119 on high PT-131 pressure).
argonne27 (CV16)	4	- A component is malfunctioning, however, there isn't enough information to identify the fault.
	5	- Instrumentation error was detected in VCT. End of diagnostics.
argonne28 (CV14 or CV22 or CV23)	4-7	- {valve 8389A, valve 8149C, valve 8160} - break between cold leg 3 and letdown heat exchanger - clogged piping between cold leg 3 and letdown heat exchanger
	8-19	- break between regenerative heat exchanger and letdown heat exchanger
	20	- End of diagnostics. Pump A inlet pressure is decreasing. (The pressure decrease is a secondary effect due to the decrease in VCT level and pressure).
argonne29 (CV01 ≡ CV29 or CV10 or CV27)	5-7	- {pump A, valve CV-121, valve 8369A, valve 8355A, seal #1, valve 8141A, valve 8112, recycle holdup tank, recycle holdup tank relief valve, seal water heat exchanger relief valve} - break between valve 8369A and pump A
	8	- End of diagnostics. SI filter pressure and valve HCV-182 inlet pressure are increasing. (These pressures should have increased early on during the transient).

Table 3.1. Expert System Diagnostic Results for the Blind Test of the CVCS (Cont'd)

Filename and (Transient Type)	Time into the Transient (s)	Diagnosis
argonne30 (CV13 or CV21 or CV25)	4-5	- {valve HCV-182} - break between junction 7 and cold leg 1 - break between valve CV-121 and SI filter
	6-22	- break between junction 7 and regenerative heat exchanger - break between valve CV-121 and SI filter
	23-28	- {valve HCV-182} - break between junction 7 and cold leg 1 - break between valve CV-121 and SI filter
	29	- End of diagnostics. Automatic control action caused the letdown heat exchanger outlet pressure and flow to vary.
argonne31 (CV14)	3	- A component is malfunctioning, however, there isn't enough information to identify the fault.
	4	- {valve HCV-182} - break between junction 7 and cold leg 1 - break between valve CV-121 and SI filter - clogged piping between junction 7 and cold leg 1
	5	- regenerative heat exchanger tube leak. End of diagnostics.
argonne32 (CV07)	4	- {pump A, valve CV-121, Si filter} - break between pump A and valve CV-121 - clogged piping between pump A and SI filter
	5-40	- {SI filter}
argonne33 (CV26)	5-40	- break between SI filter and valve 8369A
argonne34	4-8	- A component is malfunctioning, however, there isn't enough information to identify the fault.
	9	- End of diagnostics. Letdown heat exchanger outlet flow is under the influence of control action.

Table 3.1. Expert System Diagnostic Results for the Blind Test of the CVCS (Cont'd)

Filename and (Transient Type)	Time into the Transient (s)	Diagnosis
argonne35 (CV01 = CV29)	4	- {valve LCV-112B, pump A, recycle holdup tank, recycle holdup tank relief valve} - break between VCT and valve CV-121 - clogged piping between VCT and pump A
	5-40	- {pump A}
argonne36 (CV18)	5	- A component is malfunctioning, however, there isn't enough information to identify the fault.
	6	- Instrumentation error was detected in the VCT. End of diagnostics.
argonne37 (CV04 or CV05 or CV24)	10-40	- {valve PCV-131, valve TCV-129, valve 8542, valve LCV-112A} - break between letdown heat exchanger and VCT
argonne38 (CV14)	4	- {valve 8389A, valve 8149C, valve 8160, valve HCV-182) - break between valve CV-121 and cold leg 1 - break between valve CV-121 and SI filter - clogged piping between junction 7 and cold leg 1
	5	- regenerative heat exchanger tube leak. End of diagnostics.
argonne39 (CV12 or CV14 or CV22 or CV23)	4	- A component is malfunctioning, however, there isn't enough information to identify the fault.
	5-7	- {valve 8389A, valve 8149C, valve 8160, valve CV-8117, pressurizer relief tank} - break between cold leg 3 and letdown heat exchanger - clogged piping between cold leg 3 and letdown heat exchanger
	8-15	- {valve CV-8117, pressurizer relief tank} - break between regenerative heat exchanger and letdown heat exchanger
	16	- End of diagnostics. Pump A inlet pressure is decreasing. (The pressure decrease is a secondary effect due to the decrease in VCT level and pressure).

Table 3.1. Expert System Diagnostic Results for the Blind Test of the CVCS (Cont'd)

Filename and (Transient Type)	Time into the Transient (s)	Diagnosis
argonne40 (CV21)	4-40	- {valve HCV-182} - clogged piping between valve HCV-182 and cold leg 1
argonne41 (CV09)	5	- {letdown heat exchanger}. End of diagnostics.
argonne44 (CV01 = CV29 or CV10)	11-12	- {valve PCV-131, valve 8542}
		- {valve LCV-112B, pump A, valve CV-121, valve 8112, SW filter} - clogged piping between valve 8141A and pump A - clogged piping between VCT and junction 7

The remaining 3 simulations, argonne2, argonne7, and argonne44, correspond to transient CV04, i.e., divert valve LCV-112A failure. As illustrated in Fig. 2.1, valve LCV-112A is a three-way valve that is normally closed to the holdup tank branch. CV04 simulates the failure of the holdup tank branch of valve LCV-112A to close. Therefore, the simulation of CV04 requires the valve to be open to the holdup tank. If the valve is not open, nothing happens when the fault is inserted in the simulation. In the simulation of this transient presented in Chapter 2.0, we manually opened the valve 1 second before the introduction of CV04 such that after the introduction of the failure the valve would be stuck open at the defined severity.

In the simulations of argonne2 and argonne7, corresponding to 55% and 80% severity, respectively, none of the CVCS instruments varied from their corresponding steady-state values within the first 40 seconds into the transient. In the simulation of CV04 with 50% severity presented in Chapter 2.0, a number of instruments varied within the first 10 seconds. Thus, we strongly suspect that the person performing the simulations must have ignored the fact that for CV04 to be simulated it requires valve LCV-112A to be open.

Table 3.2. Summary of the Expert System Diagnostic Results and the Corresponding Identity and Severity of the 42 Simulated Transients of the Blind Test

Filename	Hypothesized Transients	Simulated Transient and Severity
Argonne1	CV04 or CV05 or CV06	CV06-60
Argonne2	–	CV04-55
Argonne3	CV01 ≡ CV29	CV29-90
Argonne4	CV10	CV10-5
Argonne5	CV04 or CV24	CV24-120
Argonne6	CV12 or CV14 or CV22 or CV23	CV12-100
Argonne7	–	CV04-80
Argonne8	CV16	CV16-04
Argonne9	CV26	CV26-50
Argonne10	CV01 ≡ CV29	CV01-100
Argonne11	CV14 or CV22 or CV23	CV22-100
Argonne12	CV13 or CV21 or CV25	CV25-98
Argonne13	CV13 or CV21 or CV25	CV13-70
Argonne14	CV07	CV07-86
Argonne15	CV04 or CV24	CV24-55
Argonne16	CV09	CV09-143
Argonne17	CV18	CV18-73
Argonne18	CV05 or CV06	CV05-460
Argonne19	CV27	CV27-60
Argonne20	CV14 or CV22 or CV23	CV22-80
Argonne21	–	CV08-315
Argonne22	CV13 or CV21 or CV25	CV13-40
Argonne23	CV14 or CV22 or CV23	CV23-80
Argonne24	CV21	CV21-95
Argonne25	CV01 ≡ CV29 or CV10 or CV27	CV27-15

Table 3.2. Summary of the Expert System Diagnostic Results and the Corresponding Identity and Severity of the 42 Simulated Transients of the Blind Test (Cont'd)

Filename	Hypothesized Transients	Simulated Transient and Severity
Argonne26	CV04 or CV05 or CV06	CV06-82
Argonne27	CV16	CV16-98
Argonne28	CV14 or CV22 or CV23	CV23-55
Argonne29	CV01 ≡ CV29 or CV10 or CV27	CV10-95
Argonne30	CV13 or CV21 or CV25	CV25-60
Argonne31	CV14	CV14-125
Argonne32	CV07	CV07-55
Argonne33	CV26	CV26-30
Argonne34	–	CV08-444
Argonne35	CV01 ≡ CV29	CV29-40
Argonne36	CV18	CV18-08
Argonne37	CV04 or CV05 or CV24	CV05-295
Argonne38	CV14	CV14-55
Argonne39	CV12 or CV14 or CV22 or CV23	CV12-230
Argonne40	CV21	CV21-07
Argonne41	CV09	CV09-74
Argonne44	CV01 ≡ CV29 or CV07 or CV10	CV04-10

Argonne44 is supposed to represent CV04 at 10% severity. Three facts seem to indicate otherwise. First, in the previous test of the ES presented in Chapter 2.0, we did simulate CV04 at 10% severity, in which case the severity was too mild to cause any instrument to vary from steady-state levels in the first 40 seconds into the transient. In argonne44, fourteen instruments varied within 11 seconds; which is inconsistent with the simulator capability to reproduce the runs. Second, the data of argonne44 shows that the level of the volume control tank (VCT) increases by 3% during the null transient. This seems to indicate that the collection time of the

data started in the middle of some other transient. Third, the level of the VCT continues to increase during the transient. That does not seem physically correct since the divert valve is located upstream of the VCT and it fails open. Another possibility is an increase in the makeup flow to the VCT. However, in argonne44 as well as in argonne2 and argonne7, the makeup flow is zero throughout the transient. For these reasons, in the determination of the blind test performance of ES, we removed these three simulations, argonne2, argonne7, and argonne44, from the set of 42 simulated transients. Our summary of the ES results was based on the remaining 39 transients.

3.3 Expert System Performance

Different criteria can be used to determine the performance of the proposed first-principles ES in this blind test. Here, we present two possibilities. In the first one, the performance of the system is determined based on the number of possible transient types hypothesized in each simulated transient. The number of transient types hypothesized for the 39 transients is presented in the second column of Table 3.2. This criterion implicitly uses the information in Table 2.2 about the possible set of transients that can be simulated. Table 3.3 summarizes the results. Each one of the six columns of the table illustrates if the transient was uniquely identified, identified as one of two, three, or four possibilities, incorrectly identified, or not identified, respectively, along with the corresponding filenames.

Nineteen transients, corresponding to 49% of the simulated transients were uniquely identified, 3 transients or 8% were identified as one out of two possibilities, 13 transients or 33% were identified as one out of three, 2 transients or 5% were identified as one out of four possibilities, and 2 or 5% were not identified. As discussed above, the two unidentified simulations, argonne21 and argonne34, refer to transient CV08 which can not be detected. Overall, the ES correctly diagnosed 95% of the transients with varying precision within the first 40 seconds into the transient and did not identify 5% of the transients. No transients were misclassified.

In the second criterion, the performance of the system was determined by comparing the number of possible component candidates (as opposed to the transient types) hypothesized by the expert system against the actual simulated component failure. This is a more meaningful criterion

Table 3.3. Summary of the Expert System Performance for the 39 Transient Events of the Blind Test Based on the Knowledge of the Possible Set of Simulated Transients

Uniquely Identified	Identified as One of Two Possibilities	Identified as One of Three Possibilities	Identified as One of Four Possibilities	Incorrect Diagnostics	No Diagnostics
19 (49%)	3 (8%)	13 (33%)	2 (5%)	–	2 (5%)
argonne3	argonne5	argonne1	argonne6		argonne21
argonne4	argonne15	argonne11	argonne39		argonne34
argonne8	argonne18	argonne12			
argonne9		argonne13			
argonne10		argonne20			
argonne14		argonne22			
argonne16		argonne23			
argonne17		argonne25			
argonne19		argonne26			
argonne24		argonne28			
argonne27		argonne29			
argonne31		argonne30			
argonne32		argonne37			
argonne33					
argonne35					
argonne36					
argonne38					
argonne40					
argonne41					

because it does not take into account the information about the set of component malfunctions that can be simulated. The component candidates hypothesized by the ES are presented in the last column of Table 3.1 and the simulated faulty component can be identified by combining the information about the simulated transient type in the last column of Table 3.2 with the description of the transients in Table 2.2.

Similar to Table 3.3, Table 3.4 summarizes the diagnostic results of the 39 transients of the blind test using the second criterion. Nineteen transients, corresponding to 49% of the simulated transients were uniquely identified, 3 transients or 8% were identified as one out of two possibilities, 8 transients or 20% were identified as one out of three, 7 transients or 18% were identified as one out of many, and 2 transients or 5% were not identified. The two unidentified transients correspond to CV08. Overall, the ES correctly diagnosed 95% of the transients within the first 40 seconds into the transient, did not identify 5%, and did not misclassify any transient. Although the percentage of correctly diagnosed transients is the same for both criteria, the distribution of the diagnosed transients in relation to the precision of the diagnostics is different.

For the 39 simulated transients of the blind test, the ES correctly diagnosed 95% (37/39) of the transients with varying precision within the first 40 seconds into the transient, and did not diagnose 5% (2/39). The two unidentified transients correspond to the same event type, i.e., CV08 - pressure transmitter failure, which is a sensor malfunction and not a component malfunction. Therefore, in all 39 transients the faulty component was either a subset of the component candidates hypothesized by the expert system or it was not identified. No transients were misclassified.

The precision of the 37 correctly identified transients varied based on two factors: the severity of the transients and the type, location, and quantity of available instrumentation. Transients with mild failure severity may not cause certain key plant parameters to vary from their normal steady-state values, precluding their usage in the diagnostics. Perfect instrumentation allows for unique diagnostics, while no instrumentation precludes any diagnostics. For instance, the existence of the correct instrument type, e.g., flow meter, pressure meter, thermocouple, in the correct location in the T-H system allows for unique diagnostics. Not so perfect instrumentation yields a

Table 3.4. Summary of the Expert System Performance for the 39 Transient Events of the Blind Test Based on the Number of Faulty Component Candidates Hypothesized

Uniquely Identified	Identified as One of Two Possibilities	Identified as One of Three Possibilities	Identified as One of Many Possibilities	Incorrect Diagnostics	No Diagnostics
19 (49%)	3 (8%)	8 (20%)	7 (18%)	–	2 (5%)
argonne3	argonne4	argonne5	argonne1		argonne21
argonne8	argonne24	argonne6	argonne18		argonne34
argonne9	argonne40	argonne12	argonne19		
argonne10		argonne13	argonne25		
argonne11		argonne15	argonne26		
argonne14		argonne22	argonne29		
argonne16		argonne30	argonne37		
argonne17		argonne39			
argonne20					
argonne23					
argonne27					
argonne28					
argonne31					
argonne32					
argonne33					
argonne35					
argonne36					
argonne38					
argonne41					

larger number of hypothesized component candidates, decreasing the precision of the diagnostics. The proposed ES alleviates the lack of perfect instrumentation which is always the case for real-world T-H systems. By inferring the trend of nonmeasured variables it produces the smallest set of possible component candidates.

The results of the blind laboratory test seem to be acceptable for an operator advisory system. Since the blind test was selected [3.1] as the first and key measure for benchmarking PRODIAG, the obtained results allow us to characterize this phase of the project as successful.

3.4 Overall Results

Table 3.5 summarizes the results of the total set of ninety-seven transient events used to V&V the ES. It combines the results discussed in Chapter 2.0 and the blind test. Forty-eight percent of the transients were uniquely identified, thirteen percent were identified as one of two possibilities, twenty-eight percent were identified as one of many possibilities, three percent were incorrectly identified and in eight percent of the transients no diagnosis was made. All misdiagnosed transients and twenty-five percent of the unidentified transients, i.e., two percent of the total transients, were related to instrumentation faults rather then component faults. Although the ES contains a limited number of first-principles rules for detecting signal faults, signal validation is beyond the scope of this CRADA. Of the remaining seventy-five percent of the unidentified events, fifty percent were related to transients simulated with small severity levels that could not be detected by the ES and the remaining twenty-five percent were not detected due to the lack of fidelity in the simulator models. The lack of fidelity was detected by the ES as an inconsistency in the data set, which caused the termination of the diagnostic session.

In summary, the first-principles ES has demonstrated that it is capable of identifying unanticipated events when limited plant instrumentation is available. The diagnosis capability decreases with decreasing numbers of available instruments (as expected) and with decreasing severity of the component fault. Mild transients, with small severity levels may not be detected by the diagnostic system due to the lack of available signature in the data.

Table 3.5. Summary of the Expert System Results for the Total Set of 97 Transient Events of the Braidwood Chemical and Volume Control System

Uniquely Identified	Identified as One of Two Possibilities	Identified as One of Many Possibilities	Incorrect Diagnostics	No Diagnostics
46 (48%)	13 (13%)	27 (28%)	3 (3%)	8 (8%)

3.5 Future Work

Future work shall include testing of the ES to diagnose malfunctions in different T-H systems, e.g., Component Cooling Water, Residual Heat Removal, consisting of fluid properties similar of that of the CVCS in a blind-blind test. In such a test, the ES will be provided only with the T-H system P&ID and a data set of simulated transient events and will be asked to identify the simulated component faults in the data set. The possible locations, types, and severities of the transient events will not be provided until after the analysis. A blind-blind test is rather challenging. However, if successful, it would demonstrate another unique feature and advantage of the developed diagnostic system, by showing that the PRODIAG ES methodology is indeed generic and portable to other T-H systems.

Future work shall also include an extension of the developed ES to account for T-H processes utilizing two-phase flow, multiple component failure and implementation of signal processing techniques such as low frequency bandpass filter to handle noisy signals in the determination of signal trends.

REFERENCES

3.1 ANL/CRC/ComEd CRADA Working Group Meeting, 10 December, 1993.

4.0 NEURAL NETWORK VERIFICATION AND VALIDATION

This chapter contains a detailed description of the application of the component-characteristics approach to the diagnostics of a subsystem of the Braidwood CVCS. The contents of this chapter are the following: Section 4.1 describes the subsystem of the CVCS used as a test bed for the NN approach together with a summary of the distinctive signatures of the plant-level malfunctions for this plant configuration. Section 4.2 presents a description of the transient data base available for testing the method and Section 4.3 discusses the verification of the theory presented in Chapter 4.0 of Volume 1. Sections 4.4 and 4.5 present the implementation and validation, respectively, of the technique using feedforward multilayer artificial neural networks with sigmoidal activation functions. Finally, Section 4.6 presents the conclusions and suggestions to future extensions of this work.

4.1 Description of the Plant Configuration

The subsystem of the CVCV of the Braidwood simulator selected to V&V the implementation of the component-characteristics NN approach for plant-level diagnostics is highlighted in Fig. 4.1. The topological configuration of this subsystem is identical to one of the several plant configurations considered in Chapter 4.0 of Volume 1 and duplicated here in Fig. 4.2. The diagram in Fig. 4.2 explicitly identifies the locations of the two flow meters, w_I and w_{II}, that are used for plant-level diagnostics and correspond to the two flow meters, FT-121 and FE-145, respectively, in Fig. 4.1. As discussed in Chapter 4.0 of Volume 1, there are seven different plant-level malfunction types that can be resolved using these two flow meters. Table 4.1 summarizes the seven malfunctions and describes the type and location of each malfunction that can be resolved with the NN approach.

With the help of Fig. 4.1, we can identify the six different segments of the configuration shown in Fig. 4.2. It follows that segment #1 corresponds to the region in Fig. 4.1 between junction No. 5 and junction No. 7 where flowmeter FT-121 is located. Segment #2 corresponds to the region between junction No. 7 and cold leg 1 of the primary system (boundary condition P_2). Segment #3 corresponds to the region between junction No. 7 and junction No. 8 where

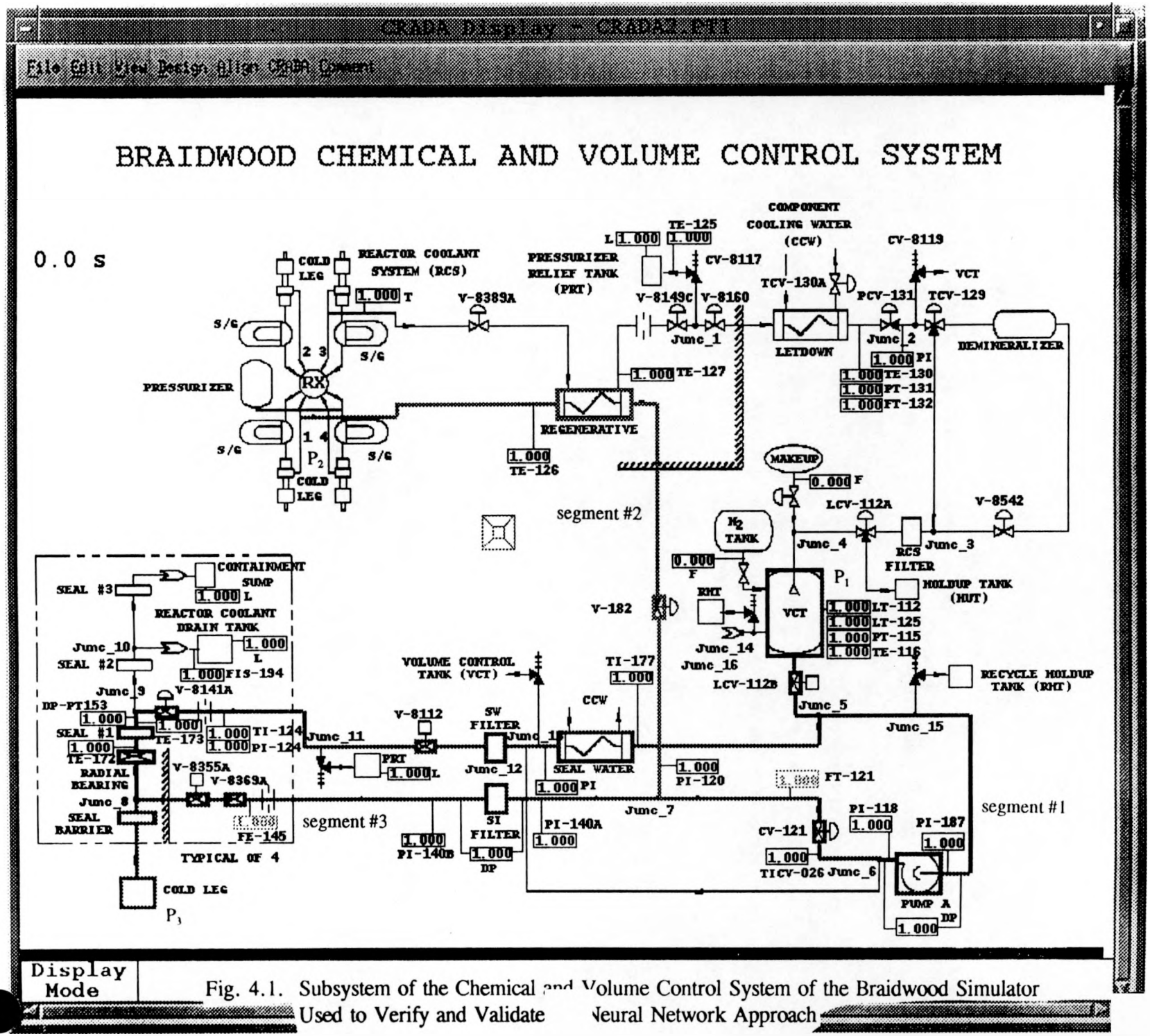

Fig. 4.1. Subsystem of the Chemical and Volume Control System of the Braidwood Simulator Used to Verify and Validate Neural Network Approach

flowmeter FE-145 is located. Segment #4 corresponds to the region between junction No. 8 and a cold leg of the primary system (boundary condition P_3). Segment #5 corresponds to the region between junction No. 8 and junction No. 5. Finally, segment #6 represents the region between the VCT (boundary condition P_1) and junction No. 5. As shown in Fig. 4.2, the closed-loop is constituted by Segments #1, #3 and #5 while the legs or branches of the loop are represented by segments #2, #4 and #6.

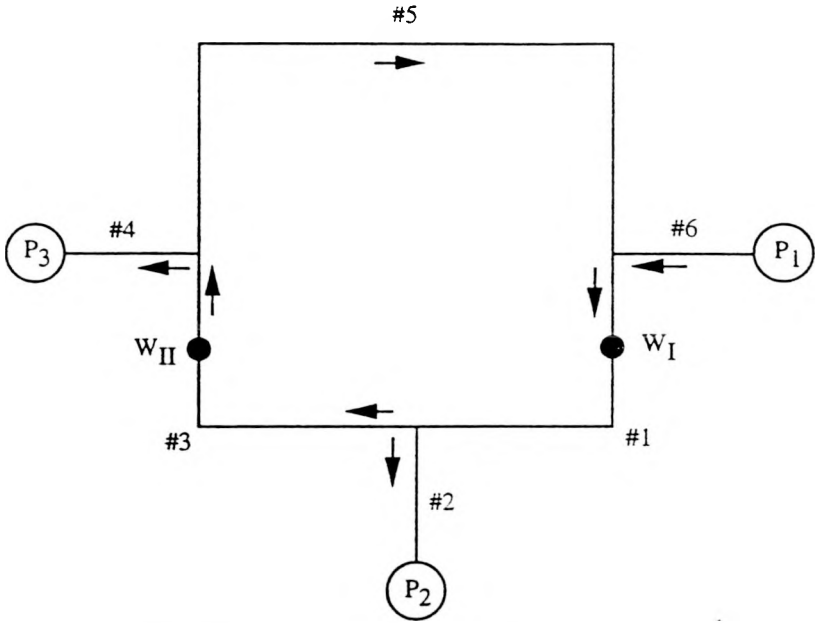

Fig. 4.2. Diagram of the Thermal-Hydraulic Configuration Used as a Test Bed for the Component-Characteristics-Based Diagnostic System

4.2 Transient Database

In spite of the fact that the NN approach can resolve seven malfunction types located in the six segments illustrated in Fig. 4.2, transient data were not available for all seven cases. Transients were available only for cases 1, 2 and 3 in Table 4.1, corresponding to malfunctions in segments #1, #2 and #3, respectively. As illustrated in Table 4.2, there is only one transient event type for each one of segments #1 and #3, and four transient event types for segment #2. Each one of the six transient event types, CV10, CV25, CV14, CV13, CV21 and CV07, is represented by three severity levels forming a data base of eighteen single-failure events (Table 2.2 provides a description of these six transients).

Table 4.1. Seven Malfunction Types for a Closed Loop Configuration with Three Boundary Conditions

1 - Momentum Malfunction in Segment #1	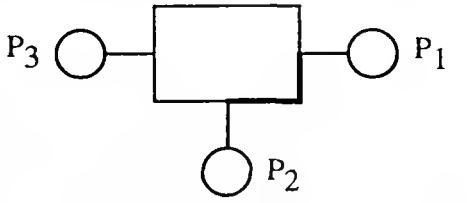
2 - Momentum or Mass Malfunctions in Segment #2 or Change in End Condition P_2	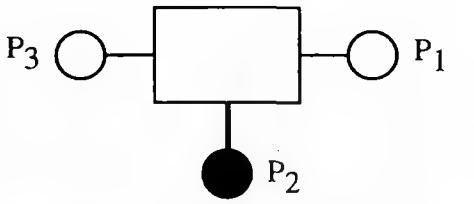
3 - Momentum Malfunction in Segment #3	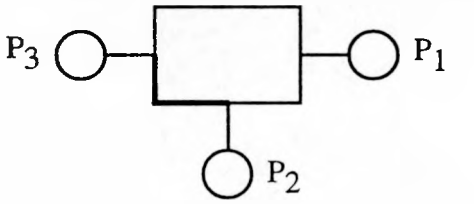
4 - Momentum or Mass Malfunctions in Segment #4 or Change in End Condition P_3	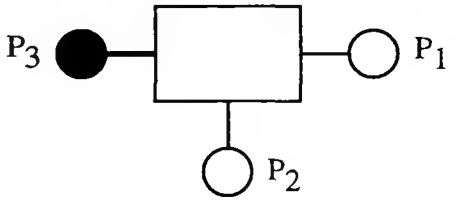
5 - Momentum Malfunction in Segment #5	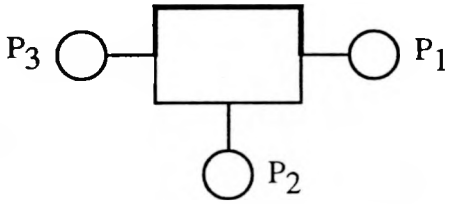
6 - Momentum or Mass Malfunctions in Segment #6 or Change in End Condition P_1	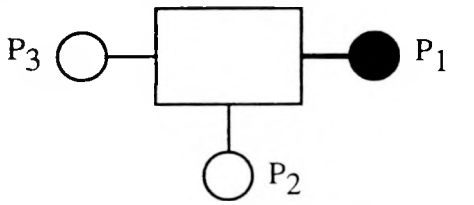
7 - Mass Malfunction in the Closed Loop	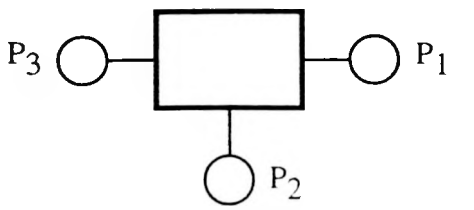

Table 4.2. Summary of Transient Events Available for Training and Testing the Characteristics-Based Neural Networks Diagnostic System

SEGMENT	TRANSIENT NAME	FAILURE TYPE
1	CV10.10	Momentum
	CV10.50	Momentum
	CV10.100	Momentum
2	CV25.10	Mass
	CV25.25	Mass
	CV25.45	Mass
	CV14.10	Mass
	CV14.35	Mass
	CV14.65	Mass
	CV13.10	Mass
	CV13.25	Mass
	CV13.45	Mass
	CV21.10	Momentum
	CV21.50	Momentum
	CV21.100	Momentum
3	CV07.10	Momentum
	CV07.50	Momentum
	CV07.100	Momentum

In the original data files of the simulated transients provided by ComEd, each event was simulated for a total of 240 seconds including 30 seconds of null-transient, i.e., steady-state normal operating conditions. From the original files of each simulated event we selected the data from the *28-th* second through the *67-th* second and constructed a new set of files consisting of only 40 seconds of data. Hence, the new data files consisted of at least 3 seconds of null-transient. From now on, all time references to transient events will be made with respect to the

new data files. This is the exact same approach used in preparing the transient data files in Chapters 2.0 and 3.0.

The transitory behavior of the simulated events died out after approximately two seconds into the transient, with the flowmeters reaching new steady-state values. To represent the initial steady-state of the six basic transient events in Table 4.2, we used six data points at 1 second and to represent the final steady-state of the eighteen transient severities we used eighteen data points at 8 seconds. Thus, the entire database consisted of 24 points (6 steady-state points at 1 second + 6 transients x 3 severity levels at 8 seconds).

4.3 Theory Verification

For the plant configuration represented in Figs. 4.1 and 4.2, the pair of flowmeters ($w_{FE\text{-}145}$,$w_{FT\text{-}121}$) is used to define the state of the subsystem. For each one of the first three segment malfunctions presented in Table 4.1, data point plots can then be made as a function of the two variables. Figure 4.3 shows the scattered plot for the three simulations of CV10 in segment #1. The point around the middle of the plot represents the steady-state values of $w_{FE\text{-}145}$ and $w_{FT\text{-}121}$ at normal operating operating conditions, that is a 1 second. The other three points correspond to measurements at 8 seconds for each one of the three failure severities of CV10 (10%, 50% and 100%). We should point out that in the simulation of certain valve failures (as is the case

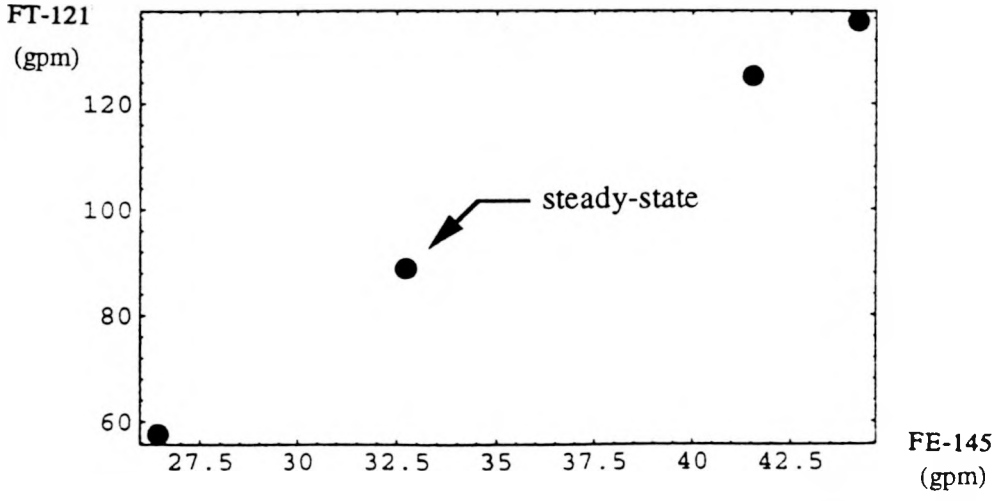

Fig. 4.3. Scattered Plot for the Simulation of Transient Event CV10 Corresponding to a Momentum Malfunction in Segment #1

for CV10) the 0% - 100% failure severity may not necessarily correspond to the magnitude of the valve travel or valve position. For CV10, a 10% failure severity causes the valve to close while 50% and 100% severities cause the valve to open. Similarly, Fig. 4.4 shows the data point plot for the transient events in Table 4.2 associated with mass and momentum malfunctions in segment #2 and Fig. 4.5 shows the plot for momentum malfunctions in segment #3.

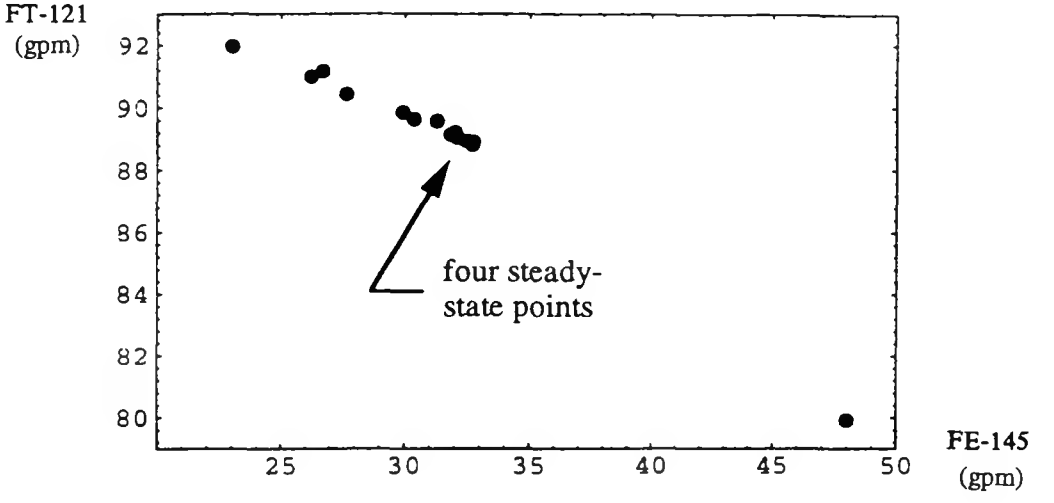

Fig. 4.4. Scattered Plot for the Simulation of Transient Events CV25, CV14, CV13 and CV21 Corresponding to Mass and Momentum Malfunctions in Segment #2

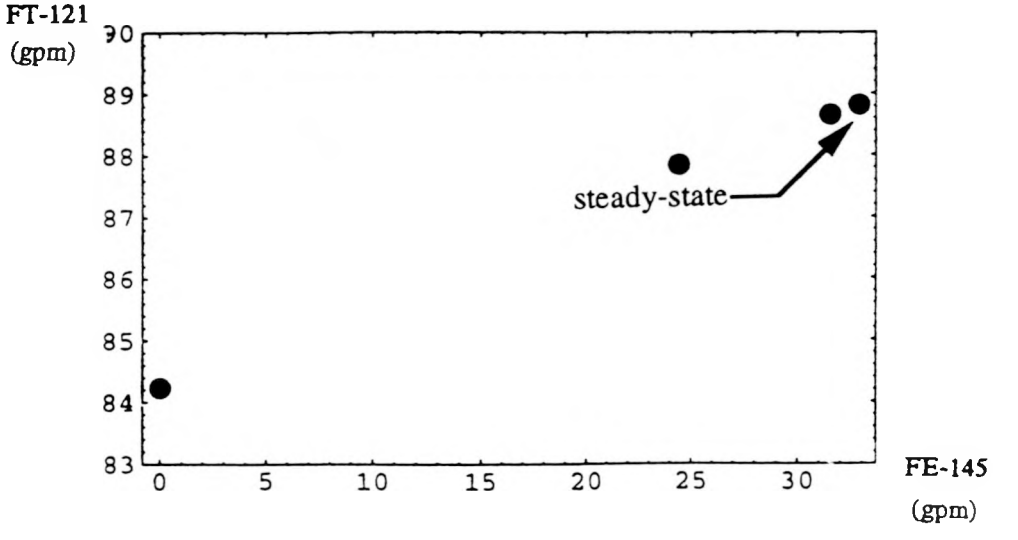

Fig. 4.5. Scattered Plot for the Simulation of Transient Event CV07 Corresponding to a Momentum Malfunction in Segment #3

Figure 4.6 shows the results of fitting the data Figs. 4.3 - 4.5 with third-order polynomials. Polynominals of third order were chosen because in the cases of Figs. 4.3 and 4.5 only four data points were available. Curve (1) is the result of fitting the scattered points in Fig. 4.3, and curves (2) and (3) are the result of fitting the scattered points in Figs. 4.4 and 4.5, respectively. As expected, the three curves intersect each other around the same point corresponding to the steady-state at normal operating conditions.

Figure 4.7 shows a close-up of Fig. 4.6 around the steady-state point. It is clear in the figure that the three curves do not intersect each other at exactly the same point, but rather, they cross each other within a small region of the state-space.

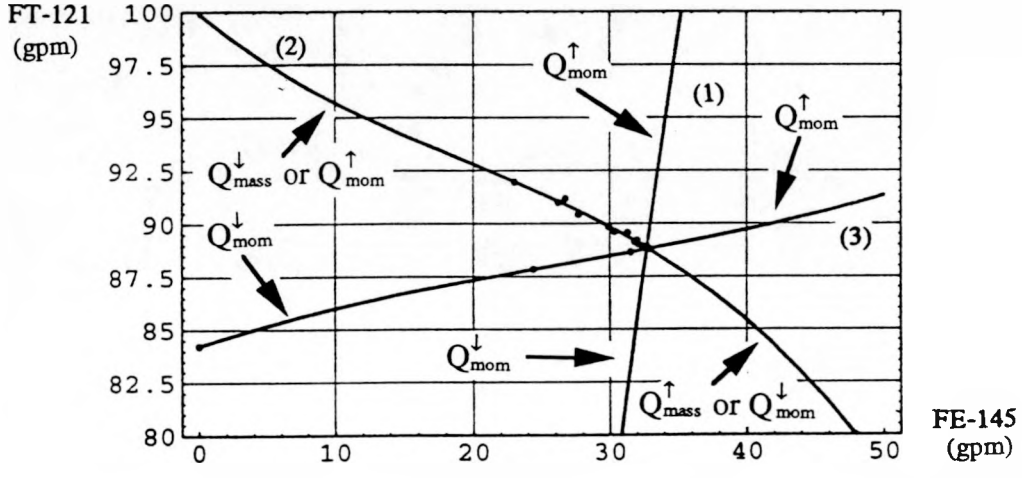

Fig. 4.6. Characteristic Curves Generated After a Least Squares Fitting of a Polynomial of Third Degree to the Data Points Shown in Figs. 4.3, 4.4 and 4.5

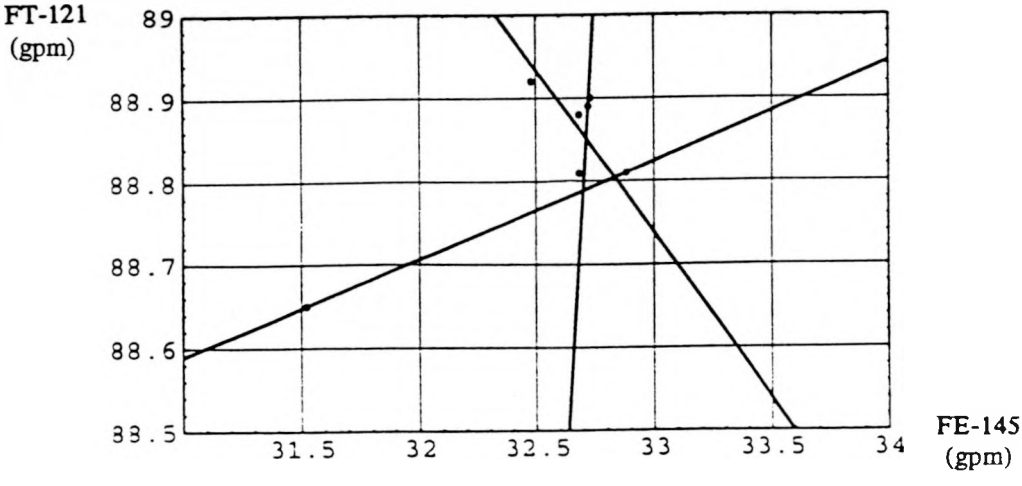

Fig. 4.7. Behavior of the Characteristic Curves Around the Steady-State Normal Operation Point

In spite of the limited number of transients available, which prevented us from studying the other segments, the results are in agreement with the behavior predicted by the theory discussed in Chapter 4.0 of Volume 1. That is, malfunctions in segments #1, #2 and #3 fall along curves (1), (2) and (3), respectively. Therefore, a momentum malfunction in segment #1 will cause the operating point of the T-H plant configuration represented in the w_{FE-145} - w_{FT-121} state-space (see Fig. 4.6) to move from the steady-state point along curve (1). The corresponding is true for malfunctions in segments #2 and #3. A momentum malfunction in segment #3 will cause the operating point to move along curve (3), while a mass or momentum malfunction in segment #2 will cause the operating point to move along curve (2).

Furthermore, the direction of the movement from steady-state along each one of the three curves indicates the imbalance direction. As illustrated in Fig. 4.6, a movement from steady-state along curve (1) in the upward direction indicates a momentum increase $Q^{\uparrow}_{mom}$ in segment #1, while a movement from steady-state in the downward direction indicates a momentum decrease $Q^{\downarrow}_{mom}$ in segment #1. Information about the imbalance direction (increase of decrease) is useful in further discriminating the faulty components through the use of the component classification dictionary (CCD) and the piping and instrumentation database (PID) just like it was applied to the ES (see Sections 2.5.2 and 2.5.3 of Volume 2). Figure 4.6 also illustrates the imbalance directions for each one of the two branches of curves (2) and (3). Table 4.3 shows the relation between the location of data points in the upper and lower branches of the three curves and the direction of the imbalances.

Table 4.3. Imbalance Direction Associated With the Lower and Upper Parts of Curves (1), (2), and (3)

SEGMENT #1 OR CURVE (1)		SEGMENT #2 OR CURVE (2)		SEGMENT #3 OR CURVE (3)	
Lower	Upper	Lower	Upper	Lower	Upper
Momentum Decrease	Momentum Increase	Mass Increase or Momentum Decrease	Mass Decrease or Momentum Increase	Momentum Decrease	Momentum Increase

Malfunctions in other segments of the plant will lie along their corresponding characteristic curves. However, due to the absence of data in those regions we were not able to obtain the curves for malfunctions in segments #4, #5 and #6.

4.4 Implementation

In this section we present the implementation of the NN approach for plant-level diagnostics using the results discussed in the previous sections. The purpose here is to train a set of NNs to identify the occurrence of five general categories of events: (a) steady-state normal operation, i.e., no fault; (b) momentum failure in segment #1; (c) mass, momentum or end condition failure in segment #2; (d) momentum failure in segment #3; and (e) mass malfunction in the loop, or a mass, momentum or end condition malfunction in segment #4 or #6, or momentum malfunction in segment #5.

In general, the events in category (e) can be separated into four different patterns corresponding to cases 4 through 7 in Table 4.1. Again, the lack of transient data prevented us from identifying these transients. Instead, these transients are lumped into one category and are identified by not belonging to the region around steady-state and not falling along any of the three curves in Fig. 4.6.

Thus, our objective in training the NNs is to partition the $w_{FE\text{-}145}$ - $w_{FT\text{-}121}$ state-space into five regions corresponding to the five categories (a) through (e). For instance, steady-state normal operation can be characterized by a small circular region in Fig. 4.7 around the intersection point of the three curves. Also, momentum failures in segment #1 can be characterized by two narrow regions surrounding the upper and lower parts of curve (1) in Fig. 4.6, with the steady-state normal operation region separating the upper from the lower part of the curve. Similar procedures can be used for categories (c) and (d).

4.4.1 Steady-State Region

The steady-state normal operating condition was obtained by averaging the maximum and minimum values of the two flow meters at 1 second, i.e., before the onset of the transients, over the six basic transient event types presented in Table 4.2. The resulting value for flowmeter $w_{FE\text{-}145}$ was 32.79 gpm and for $w_{FT\text{-}121}$ was 88.83 gpm.

All data points used in Figs. 4.3 through 4.7 can then be normalized with respect to the above values such that the normalized steady-state flowmeter values becomes the point (1,1) in the normalized state-space.

By using the same secondary threshold $\epsilon_s = 0.0045$ on the plant signals as used in the ES portion of PRODIAG presented in Section 4.4.2 of Volume 2, we can define a steady-state normal operating region in the state-space. This region is defined by the area enclosed by the circle of radius 0.0045 centered at the normalized steady-state operating point (1,1). Values of the flowmeter lying inside this region are associated with no-fault normal operating conditions, while points outside the circular region are associated with faulty conditions.

The relative small size of the steady-state region and the confluence of the three curves (see Fig. 4.6) over this region, causes the partition of the state-space by NNs to be a challenging and difficult problem. The difficulty is accentuated by 1) the fact that data values can vary by several orders of magnitude, 2) the multitude of conclusions which must be reached around the vicinity of the steady-state normal operating region are completely different from those which must be reached elsewhere in the state-space, and 3) the fact that the decision regions for categories (b) through (e) are defined by disconnected regions in state-space.

To facilitate the training of the NNs in the classification of the five categories of events we separate the problem into smaller problems. One NN is trained separately to recognize the steady-state normal operating region and each one of a set of 6 NNs is trained separately to recognize the upper and lower parts of the three disconnected curves in Fig. 4.6. Category (e) is classified by exclusion.

4.4.2 Data Preprocessing

In order to further facilitate the training of the NNs, two independent variable transformations are performed. The first transformation is used for training the NN that recognizes the steady-state region where the region is amplified by the transformation. The second transformation is used for training the other six NNs with the objective of amplifying the area surrounding the steady-state normal operating region while at the same time compressing the regions far away from the no-fault region. The two transformations are as follows:

(a) For training points used to recognize the steady-state normal operating region, each normalized flowmeter reading denoted here by x was linearly transformed using the relation

$$y = 1.0 + 100.0\ (x - 1.0)\ . \tag{4.1}$$

With this transformation, the steady-state normalized circular region of radius $r = 0.0045$ around the point (1,1) is transformed into another circular region of radius 0.45 around the point (1,1). This is, of course, simply an amplification of the steady-state normal operating region.

(b) The transformation of the data points used to recognize faulty operating conditions require a little more thought. First, we need a transformation that amplifies the region around the steady-state normal operating circular region and second, we need a transformation that compresses the outer-most regions of the state-space. Furthermore, such a nonlinear transformation should also constrain the inputs of the NNs to values between 0 and 1. For these purposes we use the following transformation:

$$y = 1 / (1 + e^{-10(x-1)})\ , \tag{4.2}$$

where x denotes the normalized flowmeter reading. This transformation maps the entire normalized state-space into a square region of side length 1, with the coordinates of the new steady-state normal operating conditions, (0.5,0.5), lying at the center of the square. The sigmoid-like transformation in Eq. 4.2 allow us to amplify the center while at the same time compress the outer-most regions of the space. For example, to first order, around the normal operating point (0.5, 0.5), the transformation reduces to $y = 0.5 + 2.5 (x - 1.0)$. In addition, this transformation has the advantage of providing a one-to-one invertible mapping.

4.4.3 Generation of the Training Patterns

Due to the small size of the transient database we generated the teaching patterns to be used in the training of the NNs for the normal operating conditions and transient events in the manner described below. In each case, the regions of interest were assigned high target values around 0.9 and the remaining regions in space were assigned target values around 0.1.

A. Steady-State Normal Operation

With the transformation in Eq. (4.1), 61 circularly symmetric input-output teaching patterns were generated to train the network to recognize the circular steady-state region. The target values (i.e., NN output training patterns) were varied smoothly from 0.9 at point (1,1) to 0.7, 0.5, 0.35, 0.25, 0.15 and 0.05 corresponding to points (i.e., NN input training patterns) 0.3, 0.45, 0.55, 0.7, 0.8 and 0.9 away from the center point (1,1), respectively. In Fig. 4.8 we show the data points that together with their associated target values were used as input-output teaching patterns for normal steady-state recognition. In the figure, FE-145* and FT-121* indicate the normalized values of the two flowmeters.

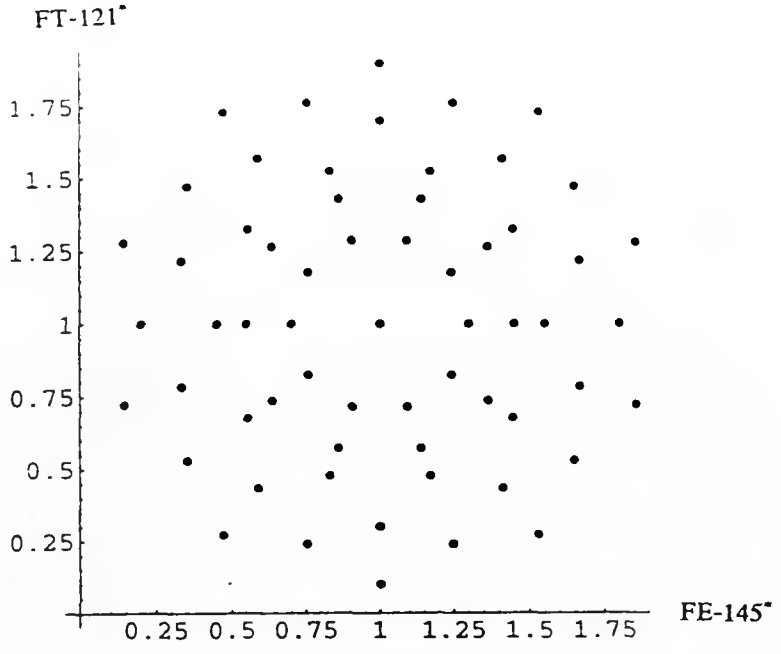

Fig. 4.8. Data Points in State-Space Used as Teaching Input Patterns to Train a Neural Network to Recognize the Steady-State Normal Operating Condition

B. Generation of Patterns for Transient Events

Before generating the data points to train the NNs to recognize the transient events, we constructed upper and lower regions associated with each one of the three curves illustrated in Fig. 4.6. With the normalization described in Section 4.4.1 such that the center of the normal steady-state region is represented by the point (1.0,1.0), but before the transformation in Eq. (4.2), and the analytical expressions for the curves obtained through the third-order polynomial fitting, we formed six disconnected regions. The regions were constructed by rotating each curve with a small angle both clockwise and counterclockwise around the (1.0,1.0) point. Figure 4.9 shows the original curves together with the new curves that form the six regions associated with the three segment faults.

The rotation angle for segment #2 was determined such that all available transient data points associated with malfunctions in this segment lie inside the constructed region. The rotation angles were found to be 3.4° clockwise and 2.6° counterclockwise. The regions associated with momentum malfunctions in segments #1 were obtained by rotating curve (1) in Fig. 4.6 by 2°

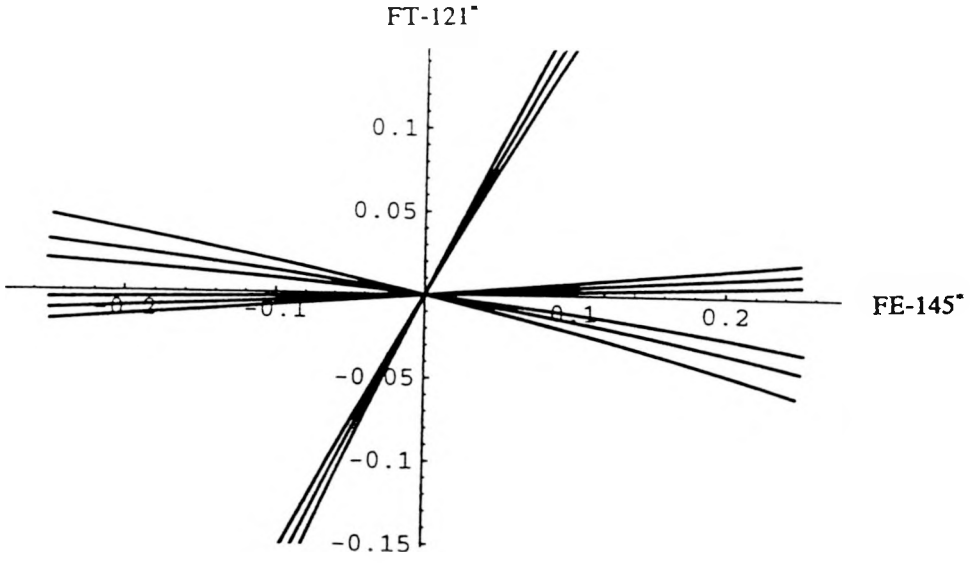

Fig. 4.9. Faulty Regions Generated by Rotating Clockwise and Counterclockwise Each One of the Characteristic Curves in Fig. 4.6 (the units indicate distances from the Normalized (1.0,1.0) normal operating point)

both clockwise and counterclockwise. Similarly, for the regions associated with momentum malfunctions in segment #3 we rotated curve (3) in Fig. 4.6 by 1.5° in each direction. These two values of the rotation angle, 2° and 1.5°, were chosen arbitrarily to form narrow but well defined faulty regions. As mentioned earlier, the upper and lower regions associated with a segment fault are separated by the steady-state normal operating region forming six disconnected regions.

For each of the six regions, the target values were selected as follows. Points along the central or original curves were associated with target values 0.95 while points along the rotated or boundary curves were associated with target values 0.5. For regions in state-space outside the six regions, various approaches were used to associate input and output pattern values. For areas neighboring each one of the six regions, points falling in a line perpendicular to the horizontal axis $w_{FE\text{-}145}$ with vertical distances $0.2\Delta w$ and $0.8\Delta w$ away from the rotated or boundary curves of each region were assigned target values 0.3 and 0.1, respectively, where Δw

is the vertical width of each region at a given $w_{FE\text{-}145}$ value. For points along the diagonal lines, i.e., $\pm 45°$, the target values were set to 0.05.

Points bordering the outside of the circular steady-state region of radius 0.0045 (after the normalization but before the transformation in Eq. 4.2) that fall along the central or original curves with distances 0.0045, 0.0065, 0.0085, and 0.01 away from the normalized center, were assigned target values 0.55, 0.75, 0.85 and 0.85, respectively. For points that also fall outside the steady-state normal operating region, but along the rotated or boundary curves with distances 0.0045, 0.0065, 0.0085 and 0.01 away from the center were assigned target values 0.7, 0.5, 0.5 and 0.5, respectively.

For points inside the steady-state circular region along the central and bordering curves we assigned a target value 0.05 for the center point, a target value 0.1 for points 0.002 away from the center and the value 0.3 for points 0.0035 away from the center.

Figures 4.10 through 4.12 illustrate the points used for training the six neural networks after the flow variables had been normalized and transformed using Eq. 4.2. We shall point out here that the selection of points falling outside the six regions played a crucial role in the accurate mapping of the entire state-space.

4.4.4 Architecture and Training

As mentioned earlier in this chapter, feedforward multilayer NNs were selected for this application. These types of networks have been extensively used in a wide variety of problems such as image and speech recognition, signal processing, power plant monitoring and diagnostics, as well as for nonlinear system identification and control [4.1, 4.2, 4.3].

Feedforward multilayer NNs are composed of many nonlinear elements or nodes arranged in layered patterns reminiscent of biological neural networks as illustrated in Fig. 4.13. In this figure $x_j^{(\ell)}$ is the activation level of the j-th node in the ℓ-th layer, determined by

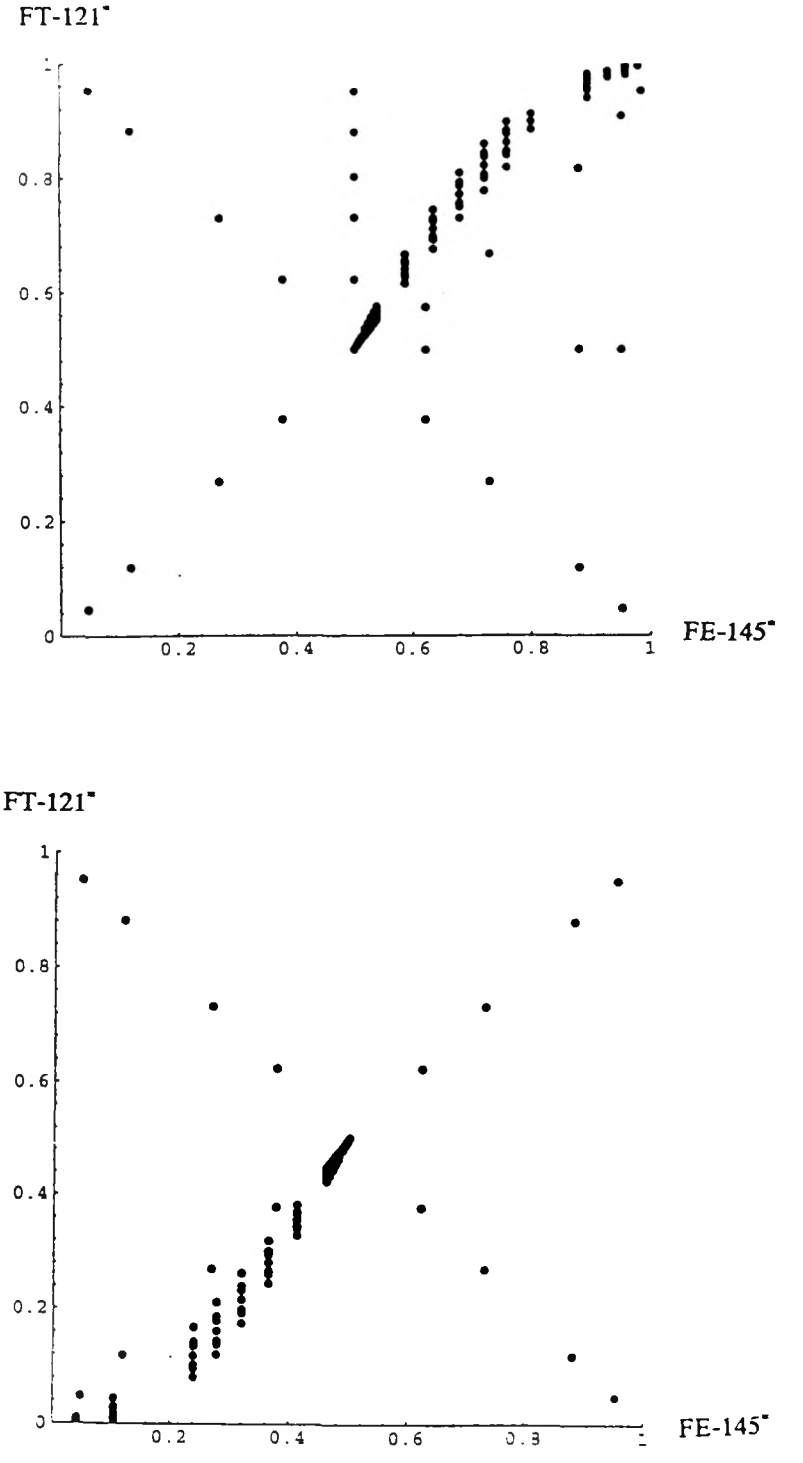

Fig. 4.10. Input Patterns Used to Train Two Neural Networks to Identify the Upper (Top Figure) and Lower (Bottom Figure) Parts, Respectively, of the Two Regions of State-Space Associated with Momentum Malfunctions in Segment #1

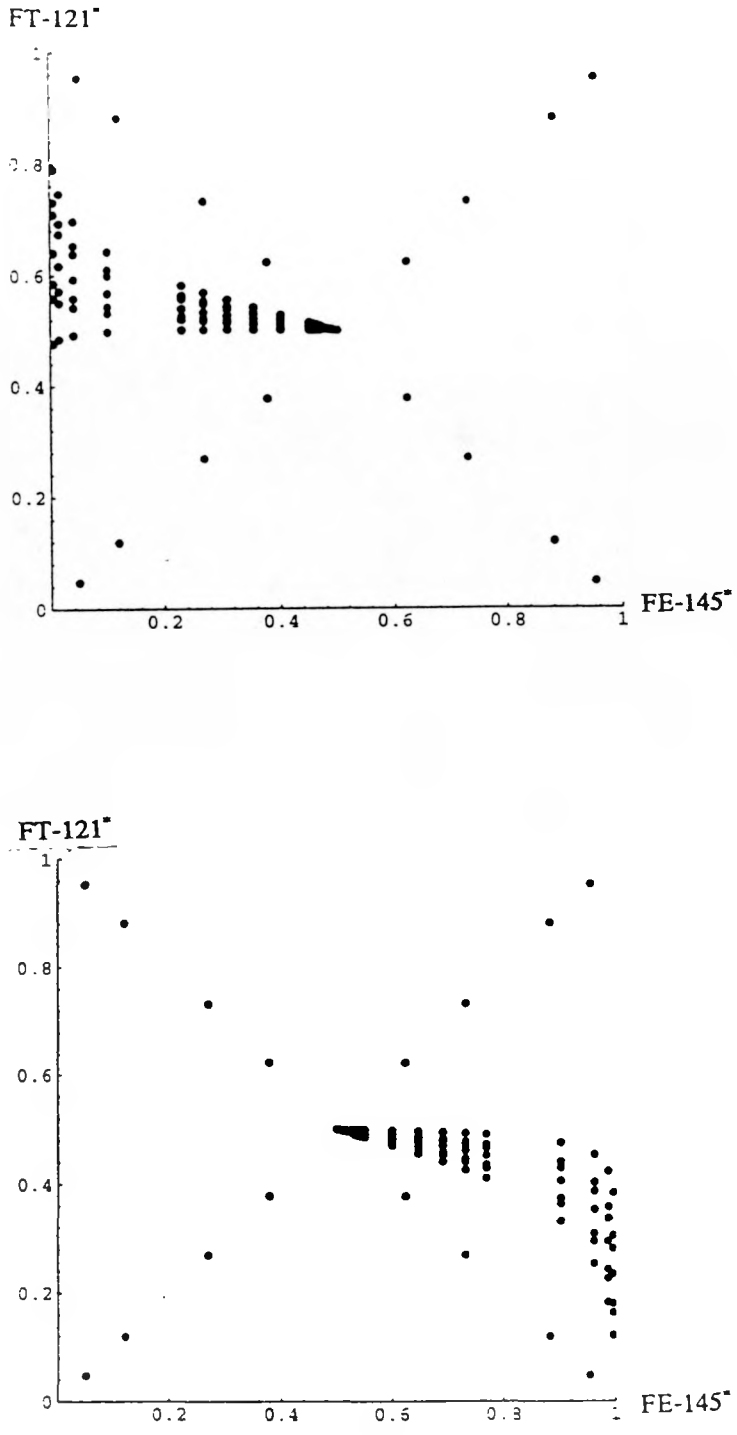

Fig. 4.11. Input Patterns Used to Train Two Neural Networks to Identify the Upper (Top Figure) and Lower (Bottom Figure) Parts, Respectively, of the Two Regions of State-Space Associated with Mass or Momentum Malfunction or Changes in the End Condition of Segment #2

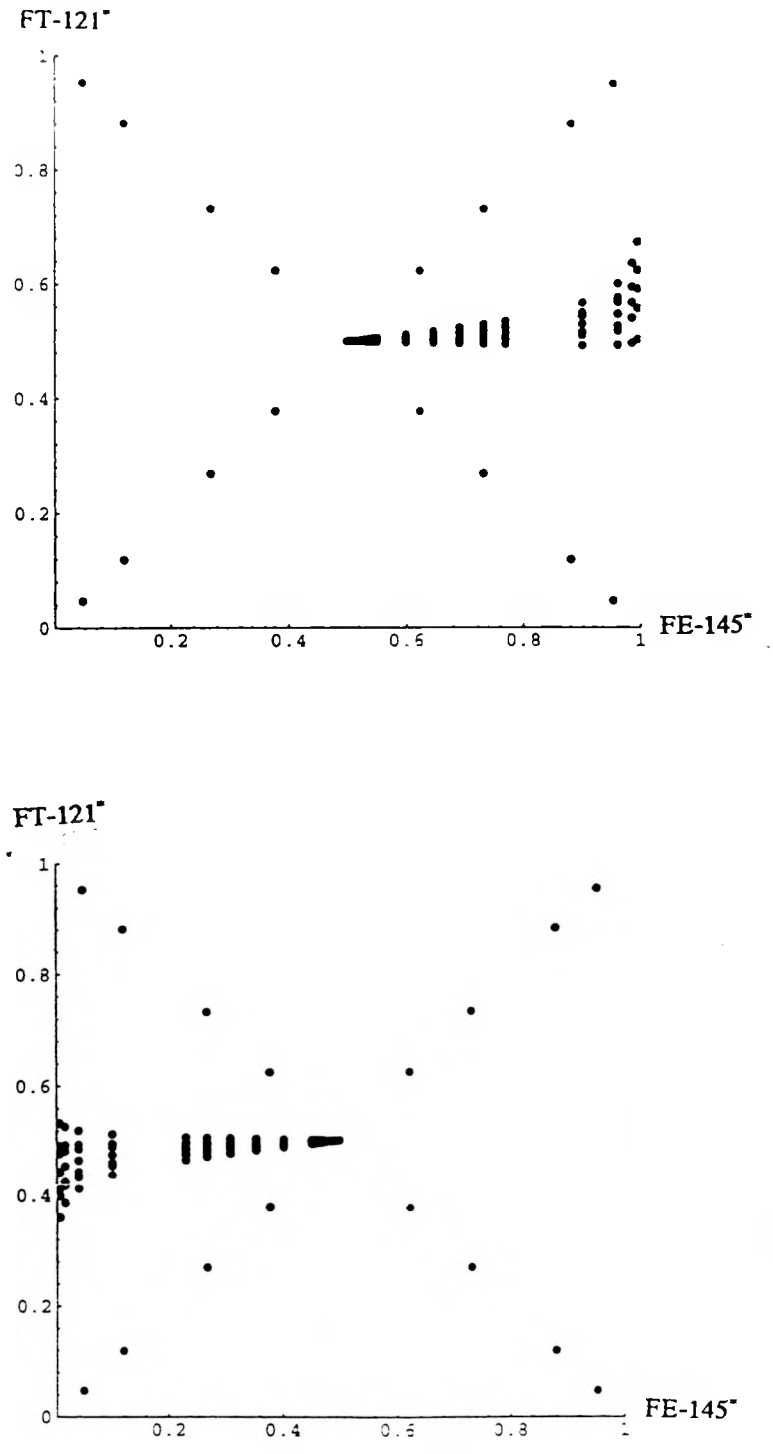

Fig. 4.12. Input Patterns Used to Train Two Neural Networks to Identify the Upper (Top Figure) and Lower (Bottom Figure) Parts, Respectively, of the Two Regions of State-Space Associated with Momemtum Malfunctions in Segment #3

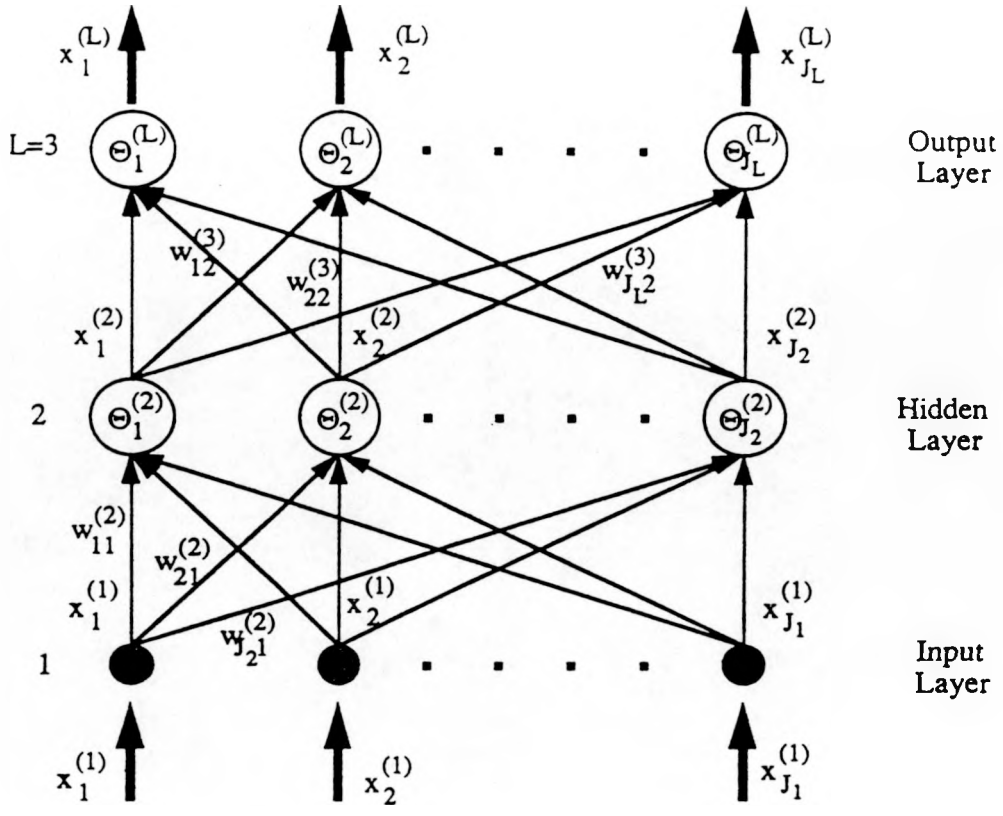

Fig. 4.13. A Typical Feedforward Three-Layer Artificial Neural Network

$$x_j^{(\ell)} = f(net_j^{(\ell)}) \,, \tag{4.3}$$

with

$$net_j^{(\ell)} = \sum_{i=1}^{J_{\ell-1}} w_{ji}^{(\ell)} \, x_i^{(\ell-1)} \,. \tag{4.4}$$

Here, $w_{ij}^{(\ell)}$ is the weight connecting the output of the *i-th* node in the *(ℓ-1)-th* layer, $x_i^{(\ell-1)}$, with the *j-th* node of the *ℓ-th* layer, $J_{\ell-1}$ is the number of nodes in the *(ℓ-1)-th* layer and $(\cdot)$ is the activation function which transforms the weighted sum of inputs, $net_j^{(\ell)}$, from layer ℓ-1 into the output of node j (see [4.4] and [4.5] for more details).

Feedforward NNs learn to produce the output associated with an input pattern from an existing database consisting of P input-output pairs of teaching patterns. Every one of these p=1, ..., P, patterns is composed of inputs $x_{pj}^{(1)}$ (j=1, ..., J_1) and target outputs t_{pj} (j=1, ..., J_L), where J_ℓ denotes the number of nodes in the *ℓ-th* layer.

The learning of the NN is accomplished by adjusting the connecting weights $w_{ji}^{(\ell)}$, so that the global error defined as

$$E = \sum_{p=1}^{P} E_p \ , \tag{4.5}$$

where

$$E_p = \frac{1}{2} \sum_{j=1}^{J_L} \left(t_{pj} - x_{pj}^{(L)} \right)^2 , \tag{4.6}$$

produced by the difference between the target t_{pj} and the actual output $x_{pj}^{(L)}$ of the NN for all P patterns is minimized.

The backpropagation (BP) algorithm [4.4] is by far the most popular method used for training feedforward multilayer NNs. The algorithm is basically an efficient method to calculate the components of the gradient E defined in Eqs. (4.5) and (4.6).

The synergism between BP and the method of conjugate gradients (CG) produced the BPCG algorithm [4.5] which has better convergence properties than the standard BP and does not require prior knowledge of the training parameters. In this work we used the BPCG algorithm for training the NNs.

It has been well established in recent years [4.1] that when the nodes are constituted by sigmoidal activation functions,

$$f(x) = 1. \ / \ (1 + e^{-x}) \ , \tag{4.7}$$

feedforward artificial networks with only one hidden layer, i.e., one layer besides the input and output layers, are capable of partitioning the state-space into convex regions. Since each one of the seven regions that we need to characterize is a convex region (i.e., every point along the line connecting any two points in the region also belongs to the region), one hidden-layer network was selected. Thus, every one of the seven networks used to partition the state-space, as described in the previous section, was designed with three layers of nodes: one input layer, one hidden layer, and one output layer. With the BPCG method, we trained the set of 7 feedforward NNs with a single layer to recognize the five different malfunctions types described in Section 4.4.1. The sigmoidal activation function was chosen such that the output values of the NNs ranged between 0 and 1.

After numerous testing of different architectures, it was found that the best NN for the characterization of the steady-state normal operating region is one that has a 2-20-1 architecture, i.e., 2 input nodes, 20 nodes in the hidden layer and 1 output node. A 2-12-1 architecture was found to be appropriate to successfully train the other six NNs to map the plant level malfunctions of categories (b) - (d). Category (e) is determined by exclusion. That is, if for a given input pattern the output or activation level of every one of the 7 NNs is below 0.5, then we infer that the input pattern is associated with fault category (e).

With the training data described in Section 4.4.3, each one of the seven NNs were separately trained. Figures 4.14 through 4.17 show the mapping of the activation levels of the output nodes of each of the seven networks for the entire state-space. Figure 4.14 (top) shows the activation level of the NN that recognizes the steady-state normal operating region and Fig. 4.14 (bottom) shows the contour plot of the activation levels. As expected the contour plots form concentric circles centered at (1,1). In this figure, activation levels of 0.5 or greater correspond to the region bounded by the circle of radius 0.45.

Figure 4.15 corresponds to the two NNs trained to recognize momentum malfunctions in segment #1 of the plant configuration in Fig. 4.2. Segment #1 corresponds to the region between junctions #5 and #7 in the diagram of Fig. 4.1. Figures 4.15 (top) and 4.15 (bottom) together constitute the malfunction regions associated with curve (1) in Fig. 4.6. Figures 4.16 (top) and 4.16 (bottom),

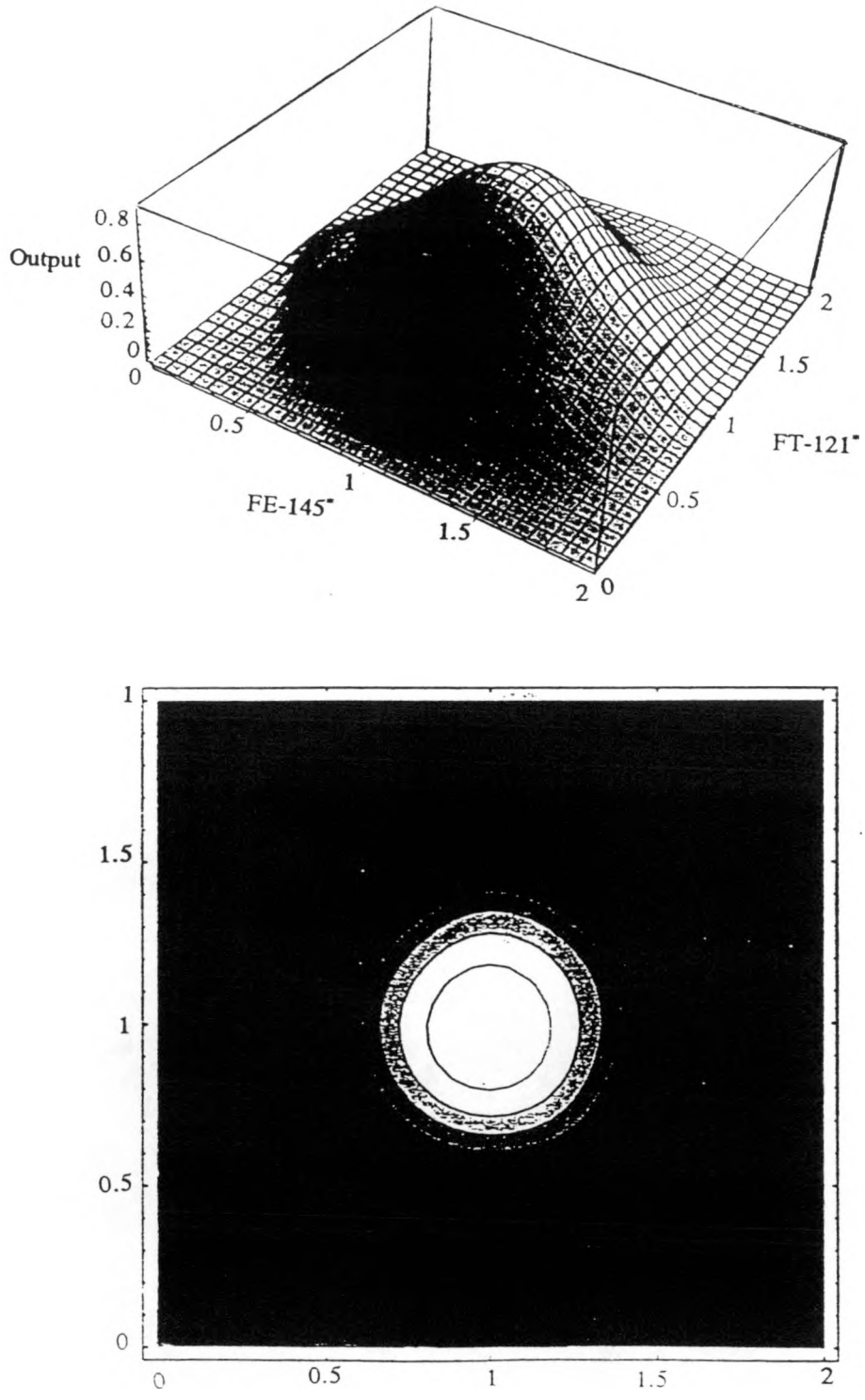

Fig. 4.14. Top: Activation Levels of the Neural Network Trained to Recognize the Steady-State Normal Operating Condition. Bottom: Contour Plot of Regions of the State-Space with Constant Activation Levels.

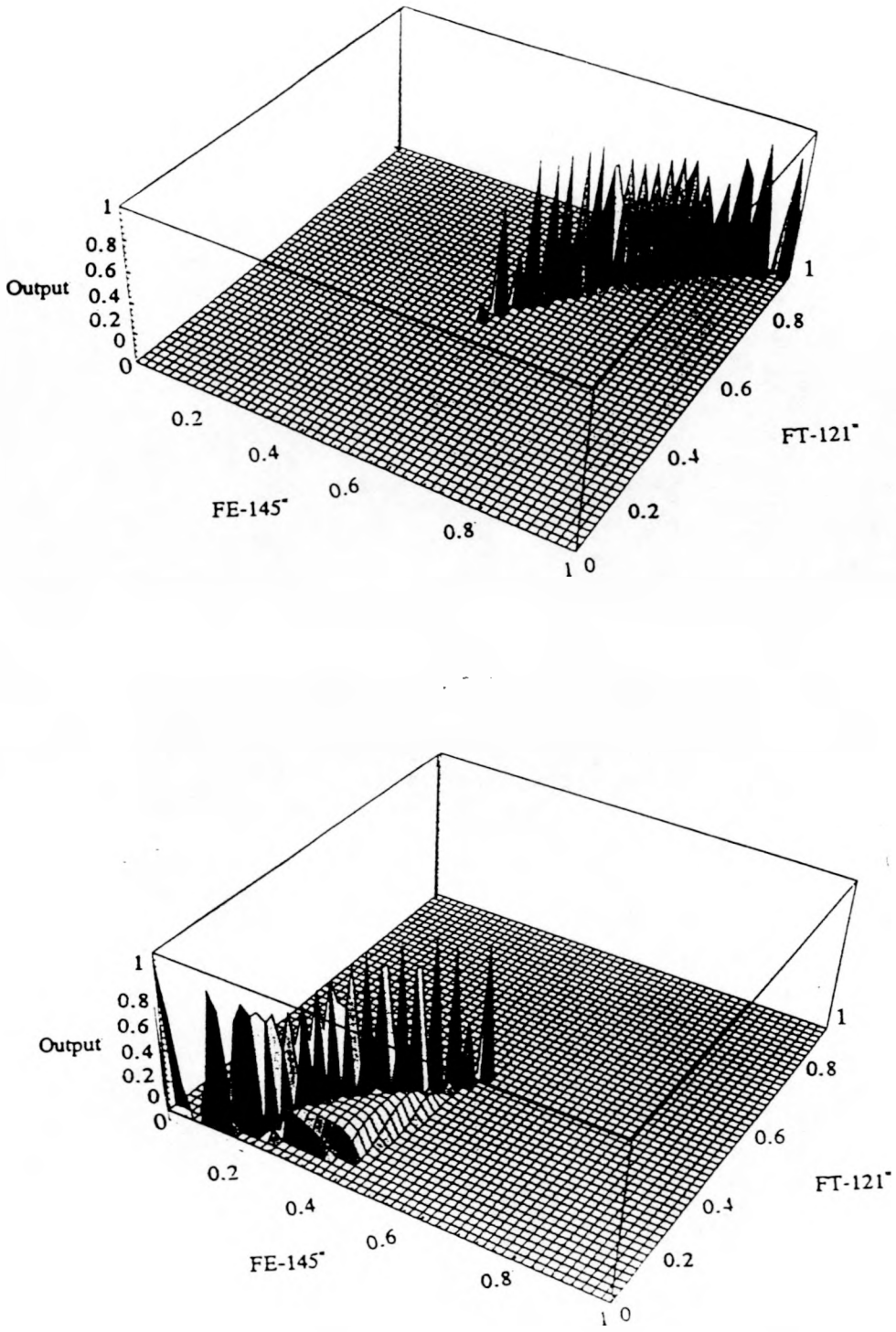

Fig. 4.15. Activation Levels in State-Space for the Two Neural Networks Trained to Recognize the Upper (Top Figure) and Lower (Bottom Figure) Parts, Respectively, of the Regions Associated with Momentum Malfunctions in Segment #1

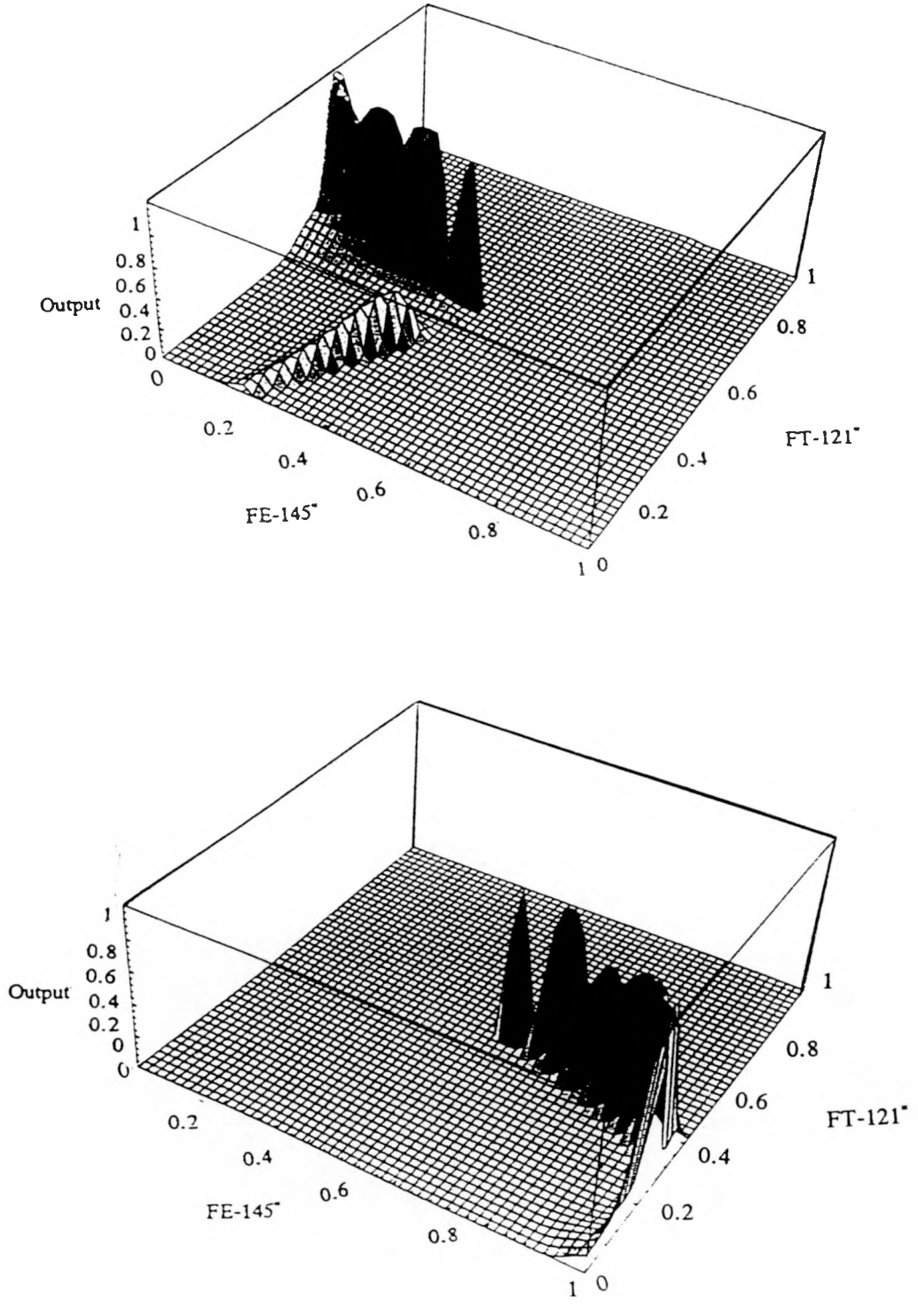

Fig. 4.16. Activation Levels in State-Space for the Neural Networks Trained to Recognize the Upper (Top Figure) and Lower (Bottom Figure) Parts, Respectively, of the Regions Associated with Mass or Momentum Malfunctions or Changes in the End Condition in Segment #2

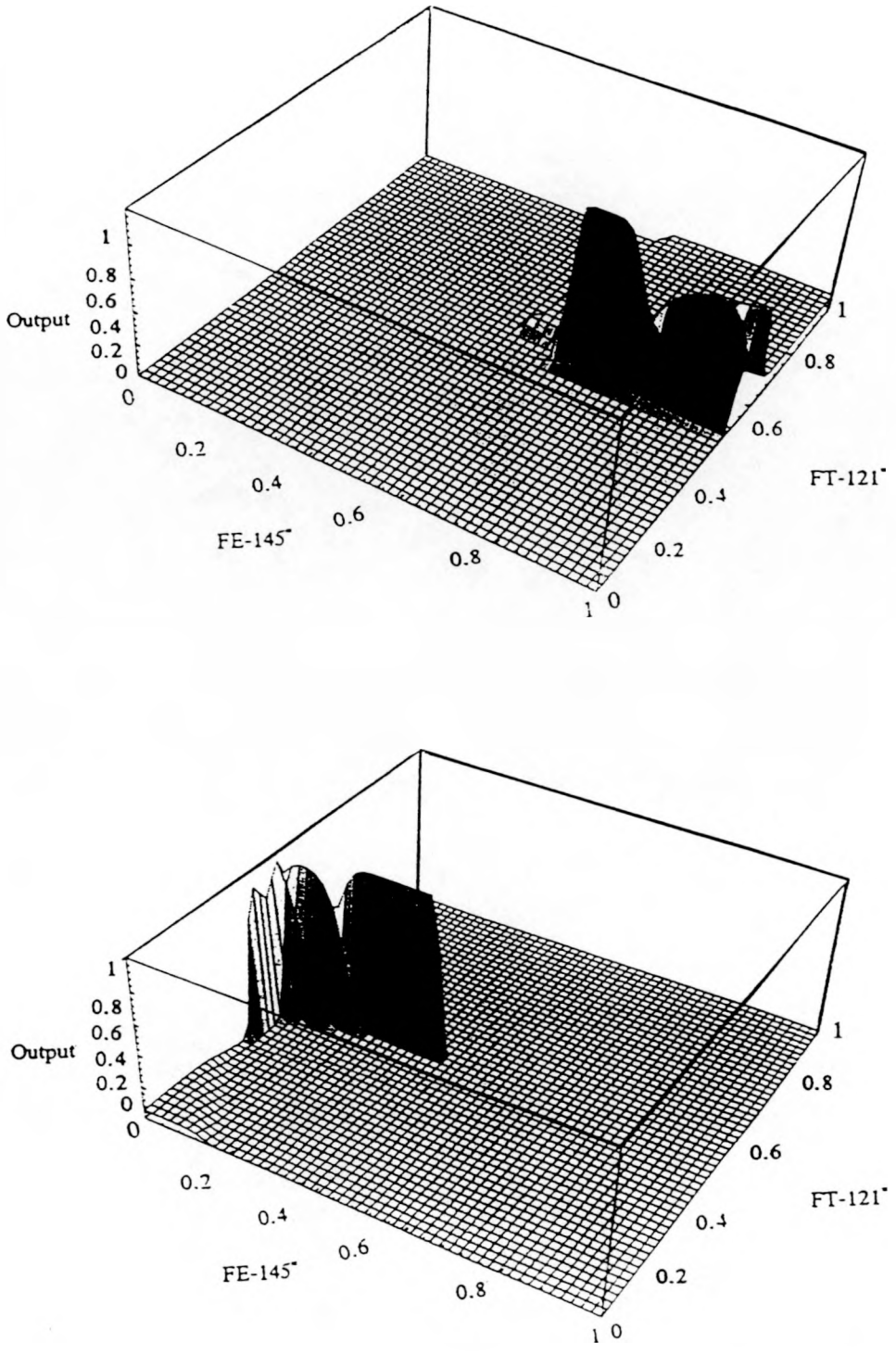

Fig. 4.17. Activation Levels in State-Space for the Two Neural Networks Trained to Recognize the Upper (Top Figure) and Lower (Bottom Figure) Parts, Respectively, of the Regions Associated with Momentum Malfunctions in Segment #3

together constitute the malfunction regions associated with curve (2) in Fig. 4.6. These regions characterize mass, momentum or end condition malfunctions in segment #2 of Fig. 4.2. This segment corresponds to the region bounded by junction #7 and the cold leg of the primary coolant system depicted in Fig. 4.1. Similarly, Figs. 4.17 (top) and 4.17 (bottom) together form the malfunction regions associated with curve (3) in Fig. 4.6. These regions characterize momentum malfunctions in segment #3 in Fig. 4.2 corresponding to the P&ID location between junctions #7 and #8.

Although this set of NNs does not reproduce exactly the target values used for training, the resulting activation levels are sufficiently close to the desired target values. However, the resulting networks can detect very reliably when a pair of flow values ($w_{FE\text{-}145}$, $w_{FT\text{-}121}$) lies inside the associated region of state-space. Figures 4.15 through 4.17 were created using Mathematica [4.6] which samples points in state-space in an attempt to represent continuous functions. Because the faulty regions are narrow, the Mathematica representation depicts anomalous spikes in the activation levels which are not present in the actual activation levels produced by the network. The spikes are the result of the sampling technique. Hence, this set of figures should not be taken as an exact representation of the input-output mapping performed by the networks, but rather as an indication of the global behavior of the output of the NNs in state-space.

We should point out here that the convergence criteria [4.5] used in the training process of these NNs was not very tight. When tight convergence criteria were used, the network learned to reproduce the training patterns better at the expense of losing the ability to correctly generalize the input-output mapping for regions which do not contain patterns used for training. Figure 4.18 shows the activation levels obtained when the NN used for characterizing the upper part of segment #1 was trained with a tighter criterion. When compared with Fig. 4.15 (top), it is evident that a tighter convergence criterion caused an undesired ridge in state-space.

To prevent the generation of undesired ridges, we trained the NNs with loose convergence criteria and also added training data outside the seven regions. For the particular case of the upper part of segment #1, a few training data were included along the vertical and horizontal lines that cross the normalized operating point. In addition, we shifted downward the input patterns along the upper

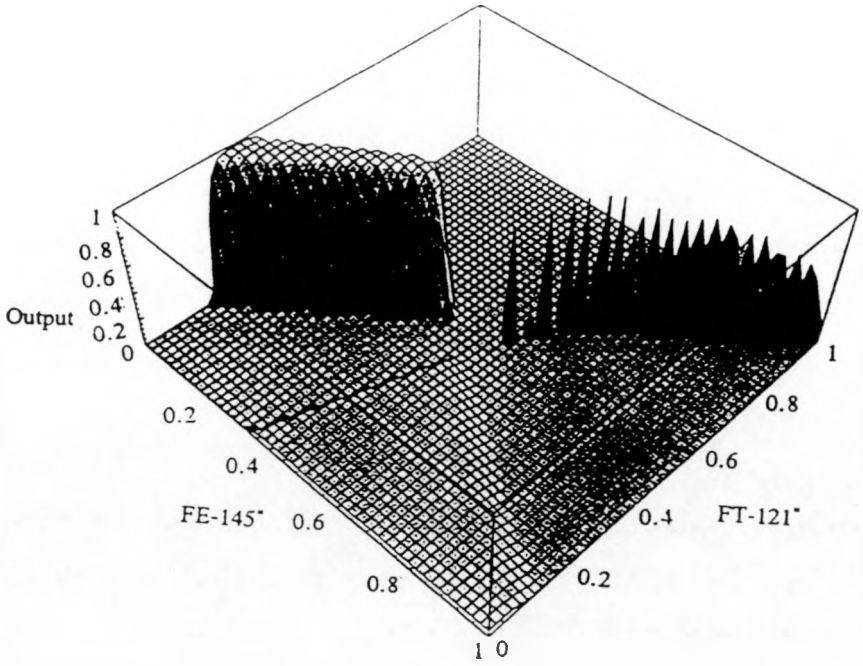

Fig. 4.18. Activation Levels for the Upper Part of Curve 1 (Segment #1) as a Function of Position in State-Space Obtained with a Tighter Convergence Criterion

right diagonal line such that these points fall outside the faulty region associated with segment #1 (see top portion of Fig. 4.10).

4.5 Neural Network Validation

In order to validate the seven NNs trained in the previous section, we used the data base of six transients presented in Table 4.2. Each one of the eighteen events in this table provided us with two validation data points, one for the steady-state condition and a second one for transient conditions. The data points used to test the steady-state condition were taken at 1 second (that is, 2 seconds before the transient starts) and the data points to test the transient conditions were taken at 5 seconds (that is, 2 seconds into the transient). Due to the short time required for the system to reach a new equilibrium point following each transport event, the two flowmeters $w_{FE\text{-}145}$ and $w_{FT\text{-}121}$ reached their asymptotic values after two seconds into the transient. The data points used to validate the networks were not used for training purposes.

Tables 4.4 through 4.9 show the validation results for the six basic transients in Table 4.2. The first column of the tables indicates the transient type and associated severity levels, e.g., CV10 at 10%,

50% and 100%. The second column illustrates the transient time which is either 1 second for steady-state or 5 seconds for transient conditions. The third column presents the values $w_{FT\text{-}121}$ and $w_{FE\text{-}145}$ for the corresponding event and transient time. The next seven columns of the tables indicate the activation levels of the output nodes of the seven NNs associated with steady-state conditions; momentum malfunctions in segment #1 (located either in the lower or upper portions of curve (1) in Fig. 4.6); mass or momentum malfunctions in segment #2 (located either in the lower or upper part of curve (2) in Fig. 4.6); and momentum malfunctions in segment #3 (located in the lower or upper portions of curve (3) in Fig. 4.6). Table 4.3 illustrates the results for data points associated with events in segment #1, Tables 4.4 through 4.7 illustrate the results for data points associated with events in segment #2 and Table 4.8 shows the results for events in segment #3.

Activation levels greater or equal than 0.50 indicate that the input data points correspond to the type of event represented by the network. For instance, the first row of Table 4.4 indicates that the flowmeter values of 88.81 and 32.70 correspond to a steady-state condition since the activation level of the steady-state network in column four, 0.74, is the only one above 0.5. Similarly, the fourth row of Table 4.4 indicates that flowmeter values 123.17 and 40.88 correspond to a momentum malfunction in segment #1 since the activation level of the network representing the upper part of curve (1) in Fig. 4.6, that is, 0.9, is the only activation level above the 0.5 threshold. As illustrated by the results in Tables 4.4 - 4.9, the trained NNs correctly and unambiguously classified all data points of the database as increases or decreases of mass or momentum. With this classification, we could then use the CCD and the PID to hypothesize faulty components just like in the ES.

4.6 Conclusions

In this chapter we have verified and validated the component characteristics approach to plant-level diagnostics using NNs for a subsystem of the Braidwood CVCS for the configuration given in Figure 4.2. It was shown that although a limited set of transient events was available in this subsystem, the results are in agreement with the theory developed in Chapter 4.0 of Volume 1. It is important to point out that although the component-characteristics plant-level diagnostic methodology is general, it is highly dependent on the instrumentation used as well as on their physical location in the plant configuration. The component characteristics approach, unlike the bulk

of the ES, needs to be customized for each particular T-H configuration. The normal steady-state operating point of the plant is also important. Changing this operating point by modifying a component in one of the segments in the plant or changing the plant state affects the location and shape of the characteristic curves in Fig. 4.6. This implies that the component-characteristics diagnostic system may have to be modified to suit the present state of the plant. Further research in this direction is necessary to address these points.

Since the ES and the NNs were both used for performing plant-level diagnosis, we now compare the two approaches with respect to ease of implementation and diagnosis resolution. Because the ES is plant-independent, except for the PID database, it is much easier to implement than the component-characteristics approach using NNs. As mentioned above, the component-characteristics approach requires a case-by-case analysis depending on the type, quantity, and location of the instrumentation in the T-H configuration to be diagnosed. In addition, if NNs are used, they need to be trained which may turn out to be a time-consuming and painstaking task.

With respect to diagnosis resolution, the component-characteristics approach yields equal or better resolution provided the same number, type, and location of instruments are used in both methods (see Chapter 4.0 of Volume 1 for an example). A one-to-one comparison between the two approaches is not relevant for the eighteen transients in Table 4.2 because in addition to the two flowmeters, FT-121 and FE-145, used in the component-characteristics approach, the ES also used pressure and temperature information. Additional information allows the ES to better discriminate the possible faulty component candidates.

If component-specific T-H data were available, the component-characteristics approach could have been used to narrow down the list of faulty components hypothesized by the ES. As described in Chapter 4.0 of Volume 1, the approach is similar to the one used here for plant-level diagnosis where the T-H characteristics of the components based on pressure difference versus flow curves or flow versus flow curves are used to detect mass and momentum imbalances. For component-level diagnosis, these T-H characteristics are used to discriminate between open valve and pump failures, and between valve A and valve B failures.

Table 4.4. Activation Levels of the Seven Neural Networks for Momentum Malfunctions (CV10) in Segment #1 of the Plant Configuration in Fig. 4.2

Transient Type and Severity	Time (Seconds)	Flowmeters w_{FT-121} (gpm) / w_{FE-145} (gpm)	Normal Operation	SEGMENT #1 OR CURVE (1)		SEGMENT #2 OR CURVE (2)		SEGMENT #3 OR CURVE (3)	
				Lower	Upper	Lower	Upper	Lower	Upper
CV10.10	1	88.81 / 32.70	0.74	4.6×10^{-8}	2.6×10^{-5}	1.5×10^{-8}	0.21	0.32	5.7×10^{-17}
	5	61.99 / 27.48	1.4×10^{-22}	0.76	4.1×10^{-62}	6.0×10^{-42}	0.01	1.3×10^{-7}	6.5×10^{-34}
CV10.50	1	88.83 / 32.70	0.74	9.3×10^{-9}	1.4×10^{-5}	1.7×10^{-8}	0.28	0.21	1.8×10^{-17}
	5	123.17 / 40.88	3.8×10^{-13}	3.1×10^{-68}	0.90	1.1×10^{-14}	8.9×10^{-20}	1.4×10^{-26}	0.09
CV10.100	1	88.86 / 32.71	0.77	1.0×10^{-8}	3.3×10^{-5}	7.1×10^{-8}	0.28	0.02	2.4×10^{-17}
	5	134.08 / 43.57	3.8×10^{-13}	5.5×10^{-68}	0.66	1.1×10^{-14}	8.4×10^{-20}	1.4×10^{-26}	0.09

Table 4.5. Activation Levels of the Seven Neural Networks for Mass Malfunctions (CV25) in Segment #2 of the Plant Configuration in Fig. 4.2

Transient Type and Severity	Time (Seconds)	Flowmeters w_{FT-121} (gpm) / w_{FE-145} (gpm)	Normal Operation	SEGMENT #1 OR CURVE (1)		SEGMENT #2 OR CURVE (2)		SEGMENT #3 OR CURVE (3)	
				Lower	Upper	Lower	Upper	Lower	Upper
CV25.10	1	88.83 / 32.68	0.66	4.8×10^{-11}	2.6×10^{-7}	3.6×10^{-10}	0.31	0.24	9.1×10^{-20}
	5	89.14 / 31.96	9.1×10^{-21}	5.3×10^{-16}	2.4×10^{-29}	1.4×10^{-22}	0.89	1.8×10^{-15}	4.1×10^{-29}
CV25.25	1	88.83 / 32.68	0.66	4.8×10^{-11}	2.6×10^{-7}	3.6×10^{-10}	0.31	0.24	9.1×10^{-20}
	5	89.51 / 31.28	1.6×10^{-20}	1.8×10^{-15}	1.4×10^{-28}	1.6×10^{-21}	0.99	1.8×10^{-9}	2.6×10^{-27}
CV25.45	1	88.82 / 32.68	0.66	1.1×10^{-10}	3.9×10^{-7}	3.5×10^{-10}	0.28	0.33	1.8×10^{-19}
	5	91.05 / 26.76	5.1×10^{-19}	7.2×10^{-14}	1.6×10^{-38}	4.5×10^{-21}	0.90	5.4×10^{-4}	5.3×10^{-27}

Table 4.6. Activation Levels of the Seven Neural Networks for Mass Malfunctions (CV14) in Segment #2 of the Plant Configuration in Fig. 4.2

Transient Type and Severity	Time (Seconds)	Flowmeters w_{FT-121} (gpm) / w_{FE-145} (gpm)	Normal Operation	SEGMENT #1 OR CURVE (1)		SEGMENT #2 OR CURVE (2)		SEGMENT #3 OR CURVE (3)	
				Lower	Upper	Lower	Upper	Lower	Upper
CV14.10	1	88.81 / 32.70	0.74	4.6×10^{-8}	2.6×10^{-5}	1.5×10^{-8}	0.21	0.33	5.7×10^{-17}
	5	88.92 / 32.50	0.08	2.6×10^{-18}	6.5×10^{-24}	3.7×10^{-21}	0.65	7.3×10^{-7}	2.15×10^{-29}
CV14.35	1	88.81 / 32.70	0.74	4.6×10^{-8}	2.6×10^{-5}	1.5×10^{-8}	0.21	0.33	5.79×10^{-17}
	5	89.03 / 32.11	2.2×10^{-20}	1.1×10^{-15}	1.8×10^{-29}	1.3×10^{-23}	0.69	3.8×10^{-14}	5.9×10^{-30}
CV14.65	1	88.86 / 32.7	0.77	1.0×10^{-8}	3.3×10^{-5}	7.1×10^{-8}	0.29	0.02	2.4×10^{-17}
	5	89.15 / 31.86	7.6×10^{-21}	7.8×10^{-16}	3.8×10^{-29}	3.3×10^{-23}	0.89	6.5×10^{-15}	7.9×10^{-29}

Table 4.7. Activation Levels of the Seven Neural Networks for Mass Malfunctions (CV13) in Segment #2 of Plant Configuration in Fig. 4.2

Transient Type and Severity	Time (Seconds)	Flowmeters w_{FT-121} (gpm) / w_{FE-145} (gpm)	Normal Operation	SEGMENT #1 OR CURVE (1)		SEGMENT #2 OR CURVE (2)		SEGMENT #3 OR CURVE (3)	
				Lower	Upper	Lower	Upper	Lower	Upper
CV13.10	1	88.85 / 32.68	0.66	9.6×10^{-12}	1.2×10^{-7}	3.3×10^{-10}	0.37	0.07	1.7×10^{-20}
	5	89.84 / 29.96	2.9×10^{-19}	4.7×10^{-14}	7.6×10^{-28}	9.8×10^{-25}	0.99	8.2×10^{-5}	5.2×10^{-27}
CV13.25	1	88.85 / 32.68	0.66	9.6×10^{-12}	1.2×10^{-7}	3.3×10^{-10}	0.37	0.07	1.7×10^{-20}
	5	90.98 / 26.24	5.1×10^{-19}	7.4×10^{-14}	2.5×10^{-39}	1.0×10^{-19}	0.96	1.2×10^{-3}	5.2×10^{-27}
CV13.45	1	88.81 / 32.68	0.66	2.4×10^{-10}	5.6×10^{-7}	3.2×10^{-10}	0.23	0.39	2.9×10^{-19}
	5	91.89 / 22.96	5.1×10^{-19}	7.4×10^{-14}	3.5×10^{-39}	1.7×10^{-29}	0.84	9.3×10^{-4}	4.8×10^{-27}

Table 4.8. Activation Levels of the Seven Neural Networks for Momentum Malfunctions (CV21) in Segment #2 of the Plant Configuration in Fig. 4.2

Transient Type and Severity	Time (Seconds)	Flowmeters w_{FT-121} (gpm) / w_{FE-145} (gpm)	Normal Operation	SEGMENT #1 OR CURVE (1)		SEGMENT #2 OR CURVE (2)		SEGMENT #3 OR CURVE (3)	
				Lower	Upper	Lower	Upper	Lower	Upper
CV21.10	1	88.80 / 32.68	0.66	5.3×10^{-10}	8.1×10^{-7}	2.8×10^{-10}	0.19	0.41	4.0×10^{-19}
	5	79.73 / 47.84	1.1×10^{-16}	4.1×10^{-13}	5.2×10^{-21}	0.83	1.1×10^{-28}	1.2×10^{-45}	1.3×10^{-7}
CV21.50	1	88.82 / 32.68	0.66	1.1×10^{-10}	3.9×10^{-7}	3.5×10^{-10}	0.28	0.33	1.8×10^{-19}
	5	89.65 / 30.40	1.7×10^{-19}	3.5×10^{-14}	5.7×10^{-28}	1.6×10^{-25}	0.99	9.0×10^{-6}	4.7×10^{-27}
CV21.100	1	88.83 / 32.68	0.66	4.8×10^{-11}	2.6×10^{-7}	3.6×10^{-10}	0.31	0.24	9.1×10^{-20}
	5	90.49 / 27.68	5.1×10^{-19}	7.3×10^{-14}	4.4×10^{-30}	1.1×10^{-26}	0.98	1.0×10^{-3}	5.4×10^{-27}

Table 4.9. Activation Levels of the Seven Neural Networks for Momentum Malfunctions (CV07) in Segment #3 of the Plant Configuration in Fig. 4.2

Transient Type and Severity	Time (Seconds)	Flowmeters w_{FT-121} (gpm) / w_{FE-145} (gpm)	Normal Operation	SEGMENT #1 OR CURVE (1)		SEGMENT #2 OR CURVE (2)		SEGMENT #3 OR CURVE (3)	
				Lower	Upper	Lower	Upper	Lower	Upper
CV07.10	1	88.82 / 32.91	0.60	3.0×10^{-15}	2.2×10^{-5}	0.26	8.5×10^{-5}	9.4×10^{-7}	0.34
	5	88.68 / 31.52	6.5×10^{-20}	3.3×10^{-14}	2.6×10^{-28}	1.9×10^{-29}	8.1×10^{-3}	0.99	1.9×10^{-22}
CV07.50	1	88.78 / 32.90	0.63	2.8×10^{-14}	2.0×10^{-5}	0.35	1.7×10^{-4}	2.4×10^{-7}	0.06
	5	87.82 / 24.41	5.1×10^{-19}	7.6×10^{-14}	2.2×10^{-39}	7.5×10^{-40}	0.07	0.98	3.4×10^{-21}
CV07.100	1	88.78 / 32.90	0.63	2.8×10^{-14}	2.0×10^{-5}	0.35	1.7×10^{-4}	2.4×10^{-7}	0.06
	5	84.10 / 0	5.1×10^{-19}	7.5×10^{-14}	1.1×10^{-39}	2.8×10^{-43}	1.6×10^{-3}	0.90	3.3×10^{-42}

REFERENCES

4.1 R. P. LIPPMAN, "An Introduction to computing with Neural Networks," *IEEE ASSP*, **4**, (1987).

4.2 E. B. BARTLETT and R. E. UHRIG, "Nuclear Power Status Diagnostics Using an Artificial Neural Network," *Nucl. Technol.*, **97**, 272 (1992).

4.3 A. G. PARLOS, A. F. ATIYA, K. T. CHONG, and W. K. TSAI, "Nonlinear Identification of Process Dynamics Using Neural Networks," *Nucl. Technol.*, **97**, 79 (1992).

4.4 D. E. RUMELHART, G. E. HINTON, and R. J. WILLIAMS, "Learning Internal Representations by Error Propagation," *Parallel Distributed Processing: Explorations in the Microstructure of Cognition*, vol. I, p. 319, D. E. RUMELHART and J. C. McCLELLAND, Eds., The MIT Press, Cambridge, Massachusetts (1986).

4.5 J. REIFMAN and J. VITELA, "Accelerating Learning of Neural Networks with Conjugate Gradients for Nuclear Power Plant Applications," *Nucl. Technol.*, **106**, 225 (1994).

4.6 WICKHAM - JONES, *Mathematica Graphics, Techniques and Applications*, Springer-Verlay, NY (1994).